

Project Labnotes

Kylie Tailin Zhu

March 22, 2020

Catch up the work done in the last term:

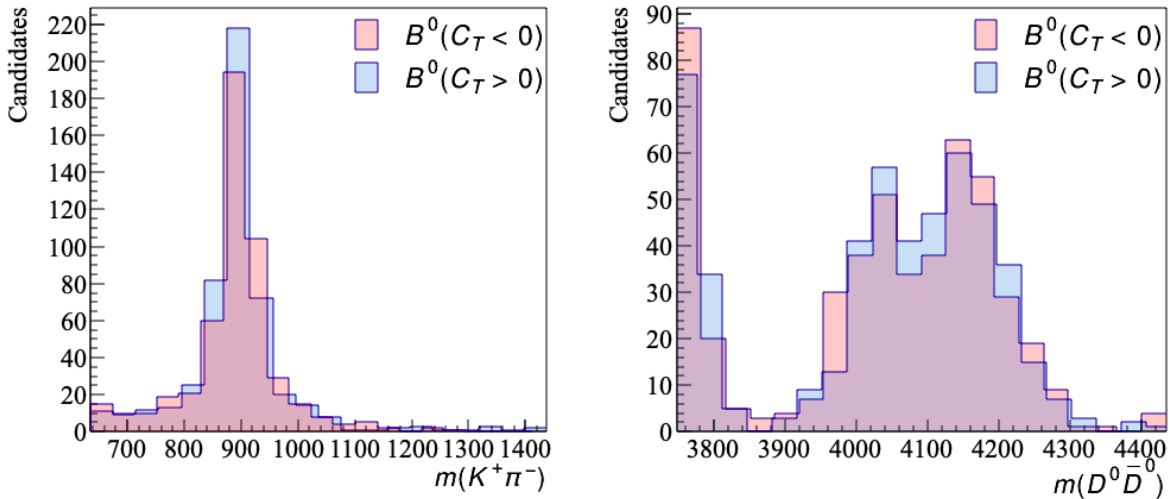


Figure 1: The binned distributions of simulated B^0 events in the variables of $m(K^+\pi^-)$ (left) and $m(D^0\bar{D}^0)$ (right) for different values of C_T .

A summary of previous work:

- Found the resonance for the $K\pi$ and $D\bar{D}$ final states with the 1000 events for the $C_T > 0$ and $C_T < 0$ cases. The data has already been in the initial frame of B^0 , so no Lorentz boost is required.
- Find the triple product asymmetry of the simulated data using $(N(C_T > 0) - N(C_T < 0))/(N(C_T > 0) + N(C_T < 0))$, which gives $(501-499)/(501+499) = 0.002$.
- calculating the invariant mass of $m(D^0\bar{D}^0K^+\pi^-)$ find that all the values equal to $5279.4 \text{ MeV}/c^2$, which is the mass of B^0 . Since all the data are generated to give this.

Next Steps:

- Find the errors in the triple product asymmetry
- Fit the binned distributions using the Breit-Wigner distributions and Poisson distribution
- Find the distribution of other CM variables

Triple Product asymmetry:

Given a Poisson distribution, the error in $N(C_T > 0)$ is simply $\sqrt{N(C_T > 0)}$ for a large number of samples, and for $N(C_T < 0)$ is $\sqrt{N(C_T < 0)}$. Denote the asymmetry A_T as

$$A_T = \frac{N_+ - N_-}{N_+ + N_-}, \quad (1)$$

I can calculate the error in A_T as

$$\begin{aligned} \Delta A_T &= \left(\frac{\partial A_T}{\partial N_+} \Delta N_+ \right)^2 + \left(\frac{\partial A_T}{\partial N_-} \Delta N_- \right)^2 \\ &= \left(\frac{2N_-}{(N_+ + N_-)^2} \right)^2 N_+ + \left(\frac{-2N_+}{(N_+ + N_-)^2} \right)^2 N_-. \end{aligned} \quad (2)$$

The result is $A_T = 0.002 \pm 0.0316$, using $C_T = \vec{p}_{K^+} \cdot (\vec{p}_{D^0} \times \vec{p}_{\bar{D}^0})$ This error is much larger than the result which indicates that no CP violation is in this sample.

Aiming to find the distribution of the five CM variables:

- the invariant masses of daughter pairs in the rest frame of the mother particle B^0 : $m(D^0\bar{D}^0)$, $m(K^+\pi^-)$
- the cosine of the helicity angles between the daughter particle and the mother-particle B^0 , in the rest frame of its daughter pairs
 - $\cos(\theta_{D^0})$ between the momentum of D^0 and B^0 in the center of mass frame of $D^0\bar{D}^0$
 - $\cos(\theta_{K^+})$ between the momentum of K^+ and B^0 in the center of mass frame of $K^+\pi^-$
 - to boost the momentum to the daughter pair rest frame:
daughter pair rest frame has four-momentum

$$\mathbf{P} = (p_{1x} + p_{2x}, p_{1y} + p_{2y}, p_{1z} + p_{2z}, E_1 + E_2) = \mathbf{p}_1 + \mathbf{p}_2, \quad (3)$$

the boost vector is then

$$\vec{V} = (p_{1x} + p_{2x}, p_{1y} + p_{2y}, p_{1z} + p_{2z})/(E_1 + E_2) = (\vec{p}_1 + \vec{p}_2)/M. \quad (4)$$

- M is not the invariant mass of the daughter pair, but the sum of the masses of two daughters, i.e. $E_1 + E_2$.
- particularly check the direction of the boost, sometimes need to add a minus sign before the boost vector
- check if the boost is correct:
 - boost the daughter pair Lorentz vector to its rest frame gives zero in the three-momentum.
 - the distribution of the $\cos(\text{angle})$ should look uniform and not peak at one side of the graph.
- the angle ϕ between the planes of the daughter pairs in the rest frame of mother particle B^0 . In this case, the between the plane $D^0\bar{D}^0$ and the plane $K^+\pi^-$.

The distributions were found with 100 bins:

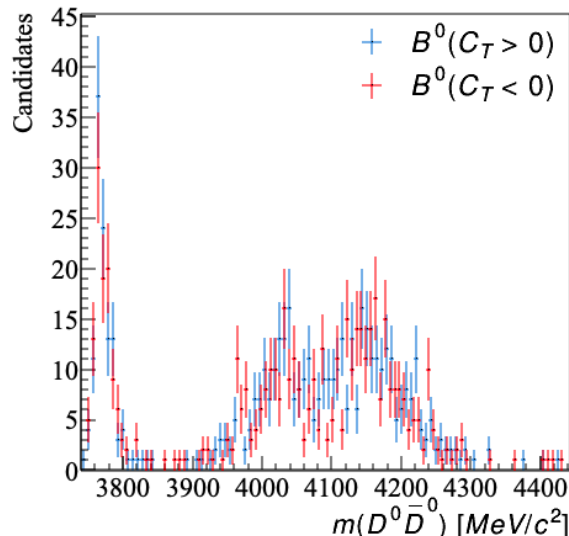


Figure 2: The binned distributions of invariant mass $m(D^0\bar{D}^0)$ for different values of C_T .

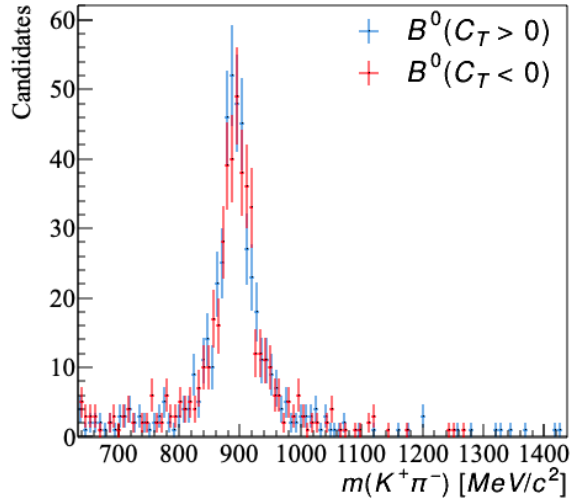


Figure 3: The binned distributions of invariant mass $m(K^+\pi^-)$ for different values of C_T .

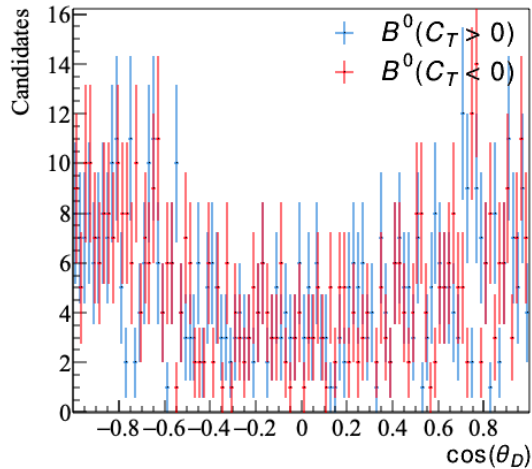


Figure 4: The binned distributions of helicity angle $\cos(\theta_{D^0})$ for different values of C_T .

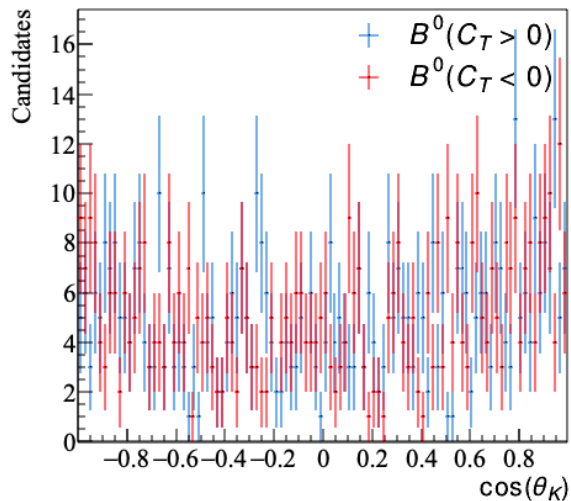


Figure 5: The binned distributions of helicity angle $\cos(\theta_{K^+})$ for different values of C_T .

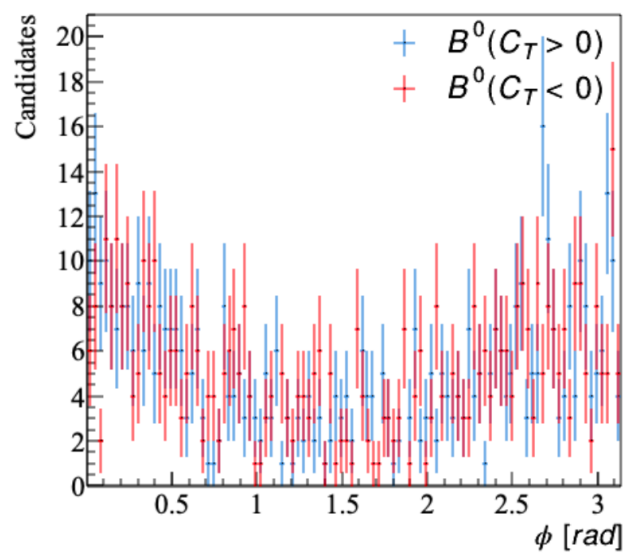


Figure 6: The binned distributions of the angle ϕ between the plane $D^0\bar{D}^0$ and the plane $K^+\pi^-$ for different values of C_T .

Fitting the invariant mass distributions using the relativistic Breit-Wigner distribution:

$$f(E) = \frac{k}{(E^2 - M^2)^2 + M^2\Gamma^2}, \quad (5)$$

$$k = \frac{2\sqrt{2}M\Gamma\gamma}{\pi\sqrt{M^2+\gamma}},$$

$$\gamma = \sqrt{M^2(M^2 + \Gamma^2)},$$

E - center of mass energy that produce the resonance,

M - mass of the resonance,

Γ - resonance width.

Fit was performed using ROOT by defining a class for the fitting function. The left and right limit of the fit was roughly approximated from the left and right ends of the peaks in the histogram. This gives individual fitting for each peak.

The fitted results are given by:

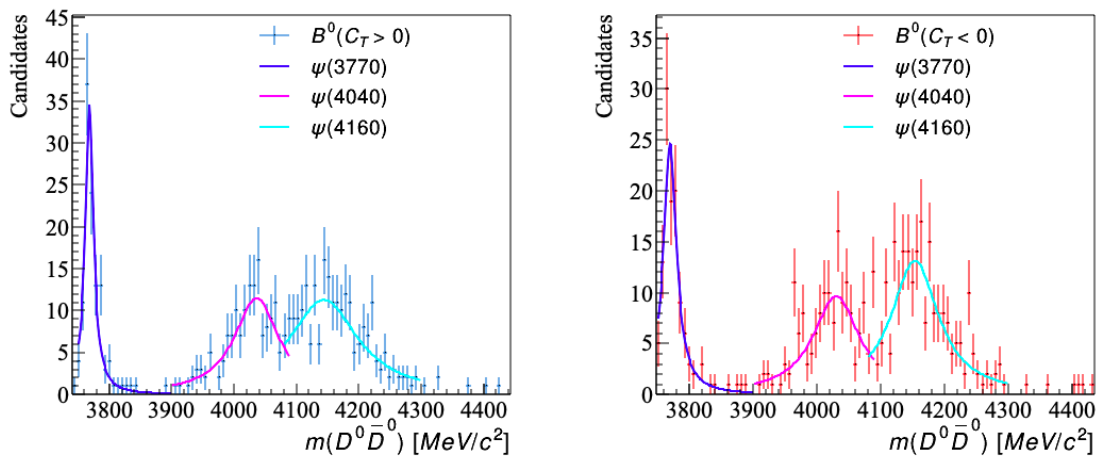


Figure 7: The binned distributions of invariant mass $m(D^0\bar{D}^0)$ for different values of C_T fitted using Eq.5

resonance	mass(M)	err_mass	width(Gamma)	err_width	Chi2	type
psi(3770)	3770	0.33	27.2	1		PDG
psi(3770)	3768.30	1.11	15.98	3.17	10.52	$C_T > 0$
psi(3770)	3769.36	1.62	24.52	3.96	8.95	$C_T < 0$
psi(4040)	4039	1	80	10		PDG
psi(4040)	4036.19	5.57	86.47	15.25	13.92	$C_T > 0$
psi(4040)	4030.10	5.21	88.63	17.02	29.27	$C_T < 0$
psi(4160)	4191	5	70	10		PDG
psi(4160)	4144.08	8.52	134.07	20.90	22.05	$C_T > 0$
psi(4160)	4153.57	4.17	90.23	11.73	30.86	$C_T < 0$

Figure 8: The fitted values from the curves in MeV

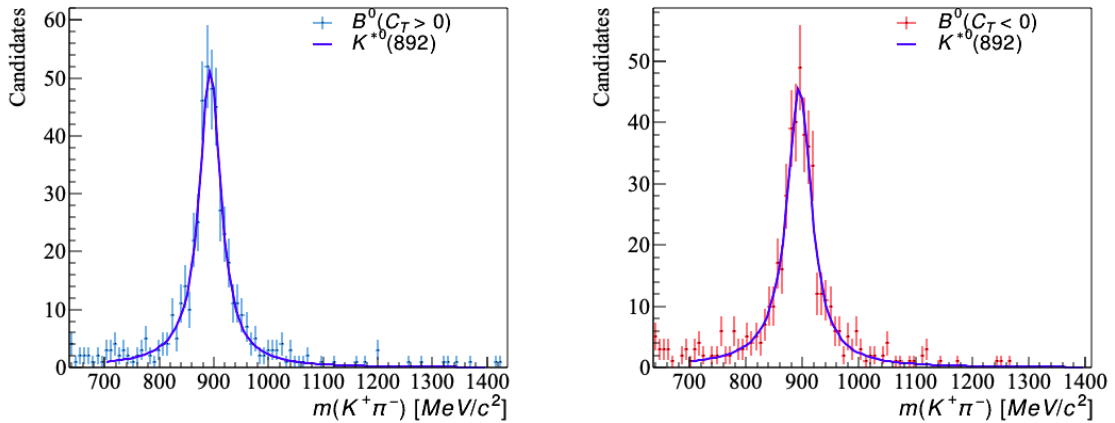


Figure 9: The binned distributions of invariant mass $m(K^+\pi^-)$ for different values of C_T fitted using Eq.5

resonance	mass(M)	err_mass	width(Gamma)	err_width	Chi2	type
K*0(892)	895.55	0.2	47.3	0.5		PDG
K*0(892)	893.52	1.53	48.07	3.55	37.29	$C_T > 0$
K*0(892)	894.35	1.65	52.39	3.90	34.30	$C_T < 0$

Figure 10: The fitted values from the curves in MeV

30 Jan 2020, Thursday

Start trying to download [AmpGen](#):

The main problem is that the AmpGen is downloaded but not be able to compile it, with the problem

```
ignoringfile/Library/Developer/CommandLineTools/SDKs/MacOSX10.14.sdk/usr/lib/libSystem.tbd, filewasbuiltforunsupportedfileformat(0x2D0x2D0x200x210x740x610x700x690x2D0x740x620x640x2D0x760x33) which  
isnotthearchitecturebeinglinked(x86_64):/Library/Developer/CommandLineTools/SDKs/MacOSX10.14.sdk/usr/lib/libSystem.tbd  
Undefined symbols for architecture x86_64:
```

One method tried:

Download a different version of the [sdk](#): MacOSX10.10.sdk.tzr.xz, which is suggested from [here](#) and [here](#).

Uncompress it to the /opt directory in the laptop:

```
sudo tar xf /Downloads/MacOSX10.10.sdk.tar.xz -C /opt
```

Add the lines into the file \$HOME/.condarc:

```
conda_build:  
  config_file:~/conda/conda_build_config.yaml
```

Here is more details of using [conda.build](#).

Then create the file \$HOME/.conda/conda_build_config.yaml and add:

```
CONDA_BUILD_SYSROOT:  
  - /opt/MacOSX10.10.sdk # [osx]
```

- But this doesn't work.

4 Feb 2020, Tuesday

AmpGen: now find a way to work from Paras - Remove everything that has been done before and follow the instructions on the installation notes.

AmpGen has been succeeded installed - now analysis the $D \rightarrow K^+K^-\pi^+\pi^-$ decay using the previous written code and check if its working correctly.

6 Feb 2020, Thursday

Outputs from AmpGen generated events:

1. $D^0 \rightarrow K^+ K^- \pi^+ \pi^-$

run the DtoKKpipi_v2.opt file

Number of Events: 171300

$$C_T = \vec{p}_{\pi^-} \cdot (\vec{p}_{K^+} \times \vec{p}_{K^-})$$

TP Asymmetry $A_T = -0.0740 \pm 0.0024$

The distributions of CM variables with 100 bins:

The distributions match the distributions in the literature, which means AmgGen can give correct results.

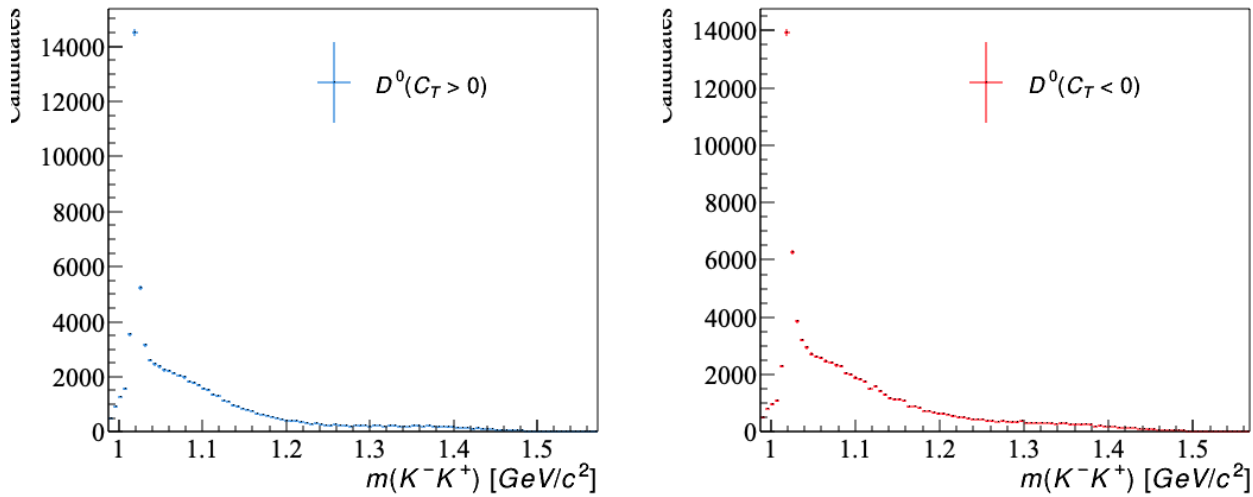


Figure 11: The binned distributions of invariant mass $m(K^-K^+)$ for different values of C_T .

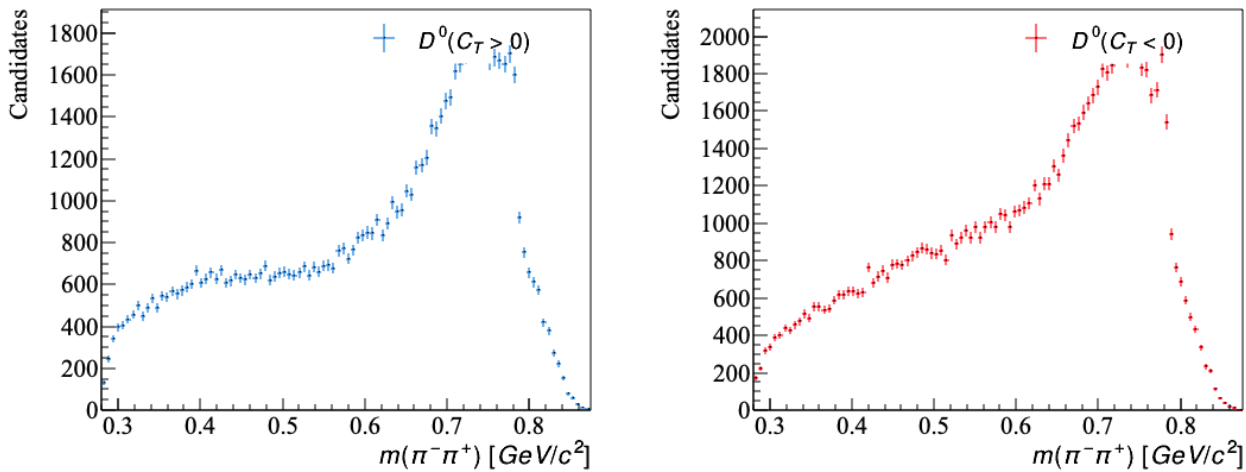


Figure 12: The binned distributions of invariant mass $m(\pi^-\pi^+)$ for different values of C_T .

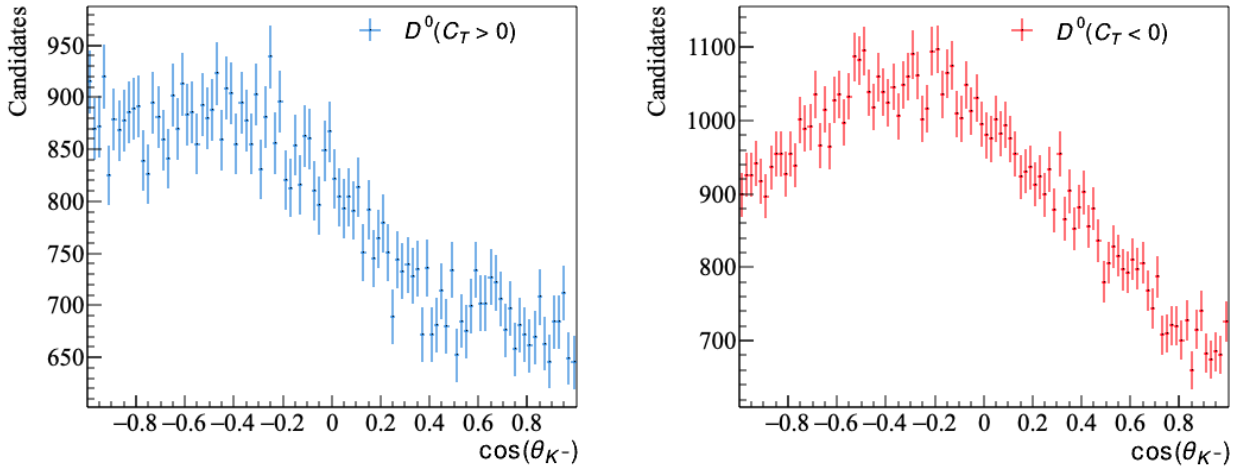


Figure 13: The binned distributions of helicity angle $\cos(\theta_{K^+})$ for different values of C_T .

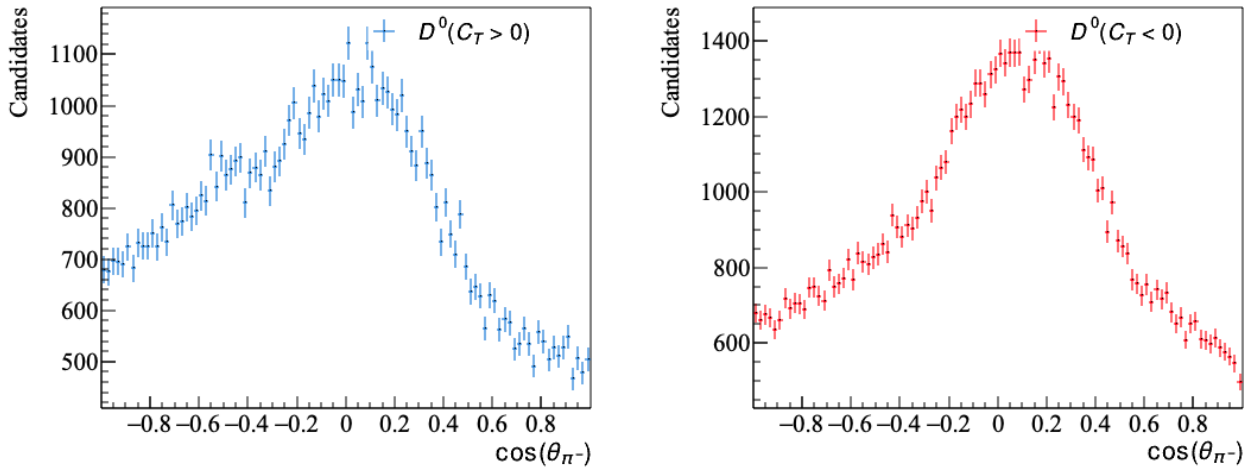


Figure 14: The binned distributions of helicity angle $\cos(\theta_{\pi^-})$ for different values of C_T .

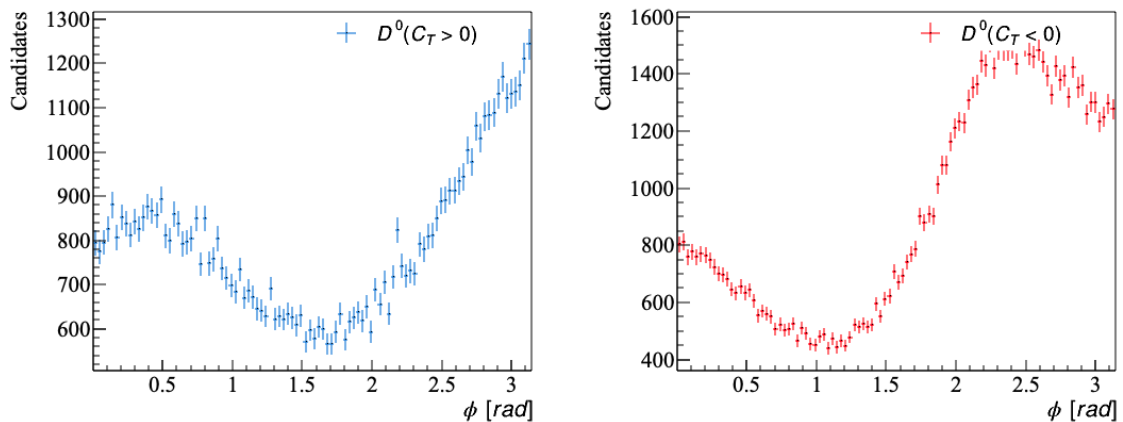


Figure 15: The binned distributions of the angle ϕ between the plane K^-K^+ and the plane $\pi^-\pi^+$ for different values of C_T .

Use AmpGen to generate $B^0 \rightarrow D^0 \bar{D}^0 K^+ \pi^-$ events.

Changes made with AmpGen:

- add B0toDDbar0K+pi-.opt file to /AmpGen/build/bin/
- inside the B0toDDbar0K+pi-.opt file, use the resonances from the MINT file (4BodyModel.txt), change the format of the resonance list and numerical values to adapt AmpGen.
- inside the B0toDDbar0K+pi-.opt file, change κ_0 to $K(0) * (800) 0$ - the particle name has been updated in PDG.
- inside the B0toDDbar0K+pi-.opt file, change the non resonance part
e.g. change $D0\bar{D}0$ to NonResS0{ $D0, \bar{D}0$ }.

From Paras: This will improve the speed considerably when including the narrow D^* resonances. It only works if all decays are done in quasi-two-body steps (i.e. $B \rightarrow \psi K^*$ as a resonance works, but $B \rightarrow D \bar{D} K^*$ doesn't)

- inside the mass_width.csv file, change line 385: J=2, P=+ for particle $D(s2)(2573)$.

2. $B^0 \rightarrow D^0 \bar{D}^0 K^+ \pi^-$

Fit the results for different events...

This still uses Eq.5 to fit but using a different approach - by summing over the Breit-Wigner functions for each peak. In this case, the events are not enough to make a clear fit for the left figure in Fig.17, the right figure in Fig.18, and the left figure in Fig.19. The fitting outcomes for resonance peaks are shown in Fig.16. For the successfully fitted peaks, it gives the expected results.

a. old results from MINT - 1000 events: $A_T = 0.002 \pm 0.0316$

bin=40 A1=45 A2=40 A3=50						
resonance	mass(M)	err M	width	err w	Chi2	type
psi(3770)	3770	0.33	27.2	1		PDG
psi(3770)	3771.31	0.67	18.29	1.91	127.20	combined
psi(3770)	3771.37	1.26	20.61	3.80	44.53	$C_T > 0$
psi(3770)	3767.06	1.29	16.95	5.06	24.09	$C_T < 0$
psi(4040)	4039	1	80	10		PDG
psi(4040)	4117.43	3.80	192.86	12.04	127.20	combined
psi(4040)	4106.79	5.85	220.99	22.96	44.53	$C_T > 0$
psi(4040)	4155.43	4.53	84.13	11.20	24.09	$C_T < 0$
psi(4160)	4191	5	70	10		PDG
psi(4160)	760.09	276.88	1.06E6	1.32E4	127.20	combined
psi(4160)	-0.09	0.50	9.92E6	2.899E7	44.53	$C_T > 0$
psi(4160)	4027.25	5.10	61.49	11.41	24.09	$C_T < 0$
K*0(892)	895.55	0.2	47.3	0.5		PDG
K*0(892)	893.33	1.15	54.14	2.74	45.24	combined
K*0(892)	892.69	1.55	51.55	3.90	17.84	$C_T > 0$
K*0(892)	897.09	311.89	0.30	311.88	367.96	$C_T < 0$

Figure 16: The fitted values from the curves in Fig.17,18,19(MeV)

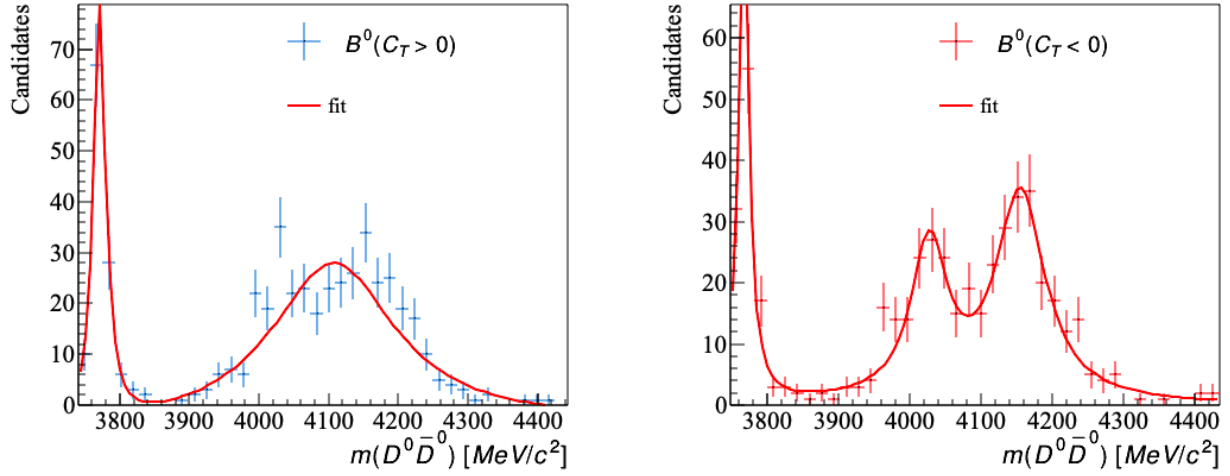


Figure 17: The binned distributions of invariant mass $m(D^0 \bar{D}^0)$ for different values of C_T .

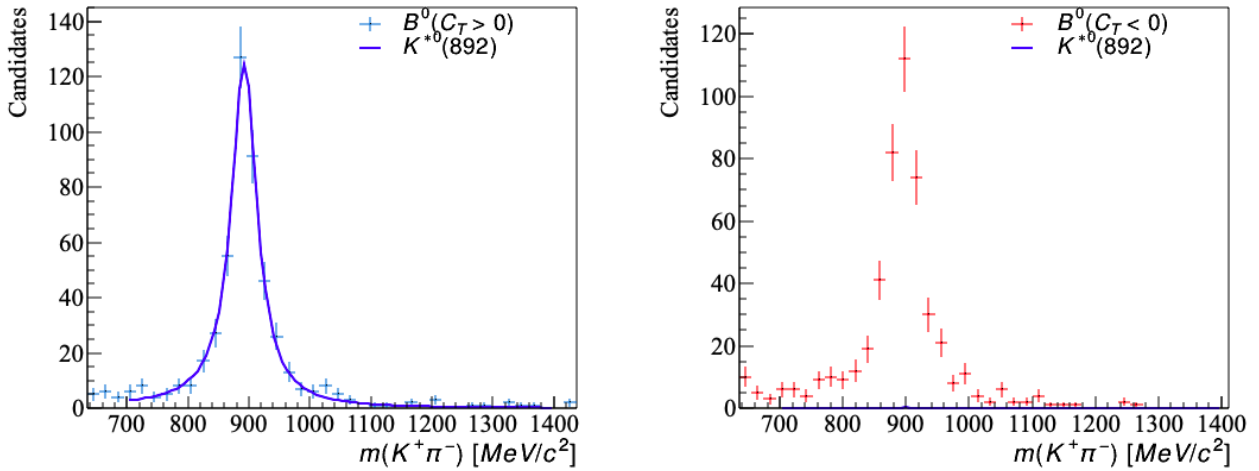


Figure 18: The binned distributions of invariant mass $m(K^+ \pi^-)$ for different values of C_T .

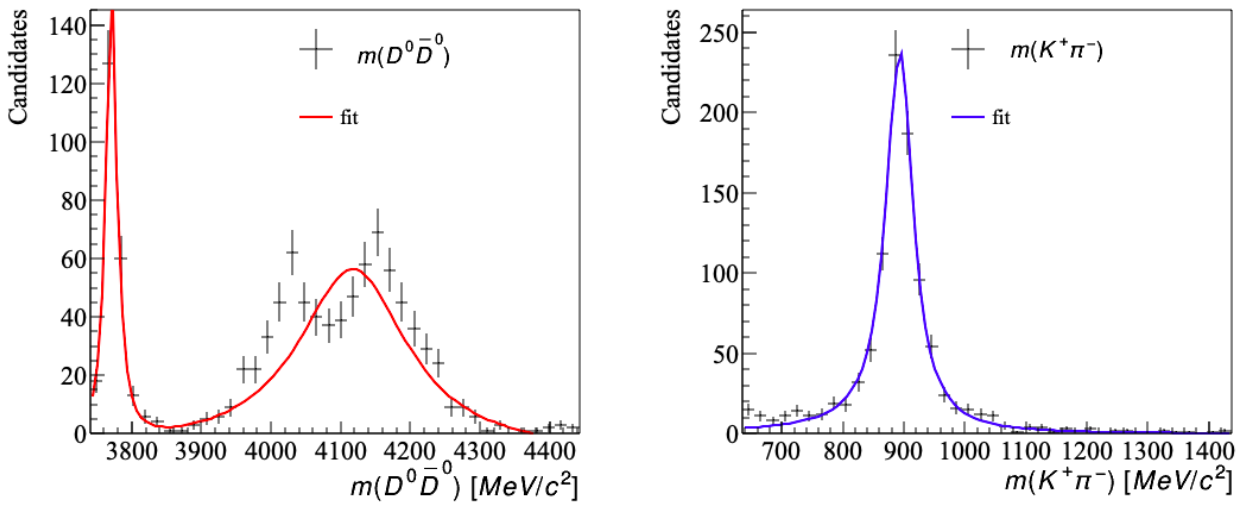


Figure 19: The binned distributions of invariant mass $m(D^0 \bar{D}^0)$ with combining data from $C_T < 0$ and $C_T > 0$.

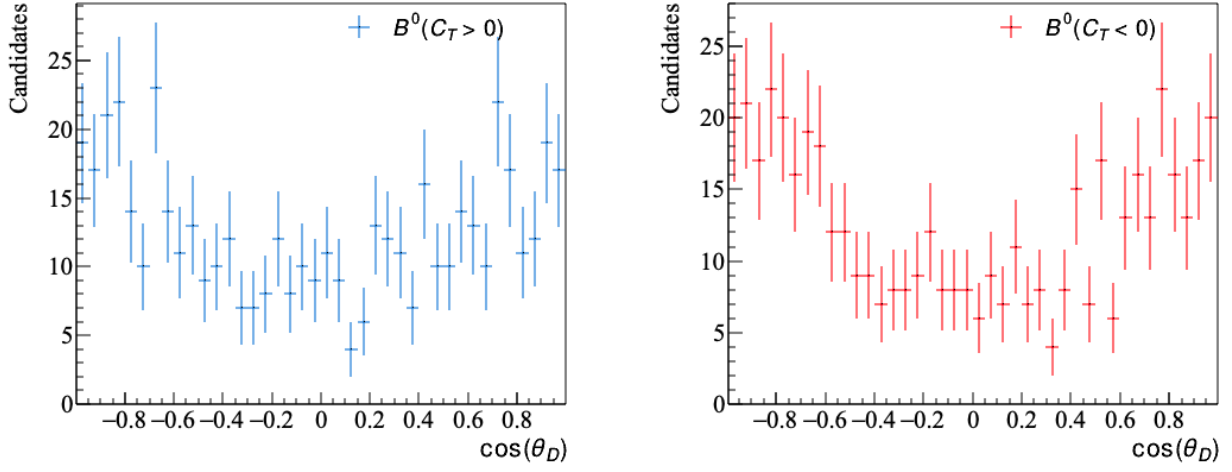


Figure 20: The binned distributions of helicity angle $\cos(\theta_{D^0})$ for different values of C_T .

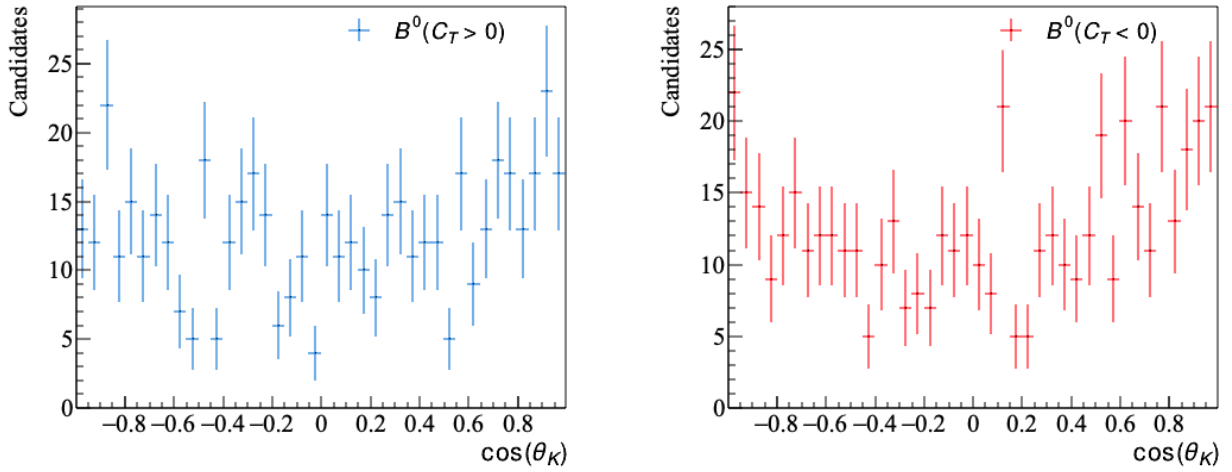


Figure 21: The binned distributions of helicity angle $\cos(\theta_{K^+})$ for different values of C_T .

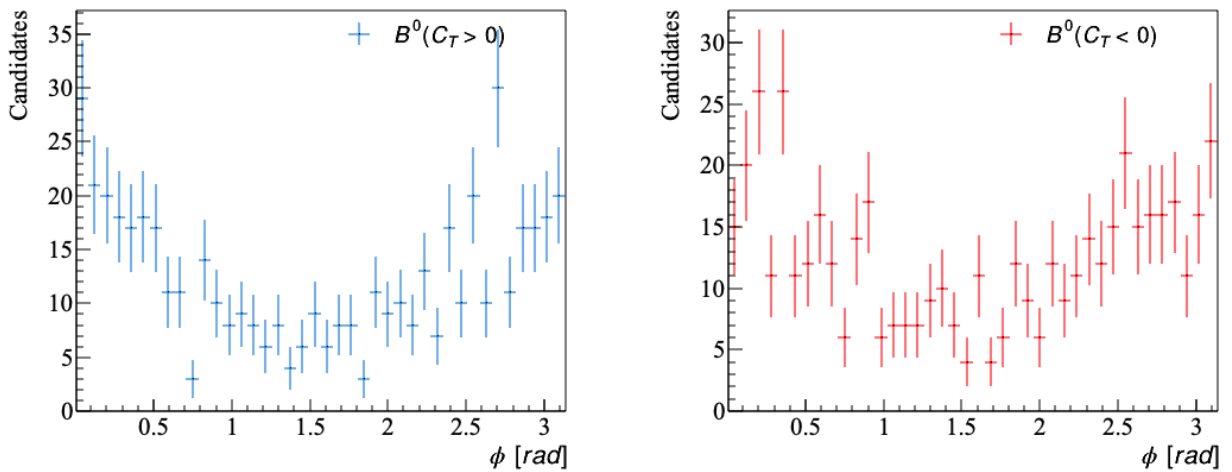


Figure 22: The binned distributions of the angle ϕ between the plane $D^0\bar{D}^0$ and the plane $K^+\pi^-$ for different values of C_T .

In order to have better fittings, more events were generated.

b. AmpGen - 10000 events: $A_T = 0.0156 \pm 0.0099987$

This fit the data properly with an increasing confident level and errors 10^2 smaller in the fitted parameters. An investigation in the confidence level of A_T , the errors in the parameters vs the number of events can be carried out.

For Fig.27, Fig.28, Fig.29, it was asked why the peaks are downwards rather than upwards in the LHCb seminar (8th Feb). It is also expected to be more flat for the helicity angles?

bin=100 A1=10 A2=10 A3=10	resonance mass(M)	err_M	width	err_w	Chi2	type	
psi(3770)	3.770	0.00033	0.0272	0.001		PDG	
psi(3770)	3.7726	0.0005	0.0236	0.0010	578.2912	combined	D0Dbar0
psi(3770)	3.7718	0.0006	0.0215	0.0014	217.7001	$C_T > 0$	
psi(3770)	3.7729	0.0007	0.0236	0.0014	243.6756	$C_T < 0$	
psi(4040)	4.039	0.001	0.08	0.01		PDG	
psi(4040)	4.0209	0.0020	0.1206	0.0049	578.2912	combined	
psi(4040)	4.0203	0.0029	0.1305	0.0086	217.7001	$C_T > 0$	
psi(4040)	4.0225	0.0031	0.1276	0.0083	243.6756	$C_T < 0$	
psi(4160)	4.191	0.005	0.07	0.01		PDG	
psi(4160)	4.1599	0.0014	0.0878	0.0028	578.2912	combined	
psi(4160)	4.1612	0.0020	0.0944	0.0047	217.7001	$C_T > 0$	
psi(4160)	4.1589	0.0022	0.0968	0.0045	243.6756	$C_T < 0$	
K*0(892)	0.89555	0.0002	0.0473	0.0005		PDG	
K*0(892)	0.8941	0.0003	0.0495	0.0008	123.0759	combined	
K*0(892)	0.8943	0.0005	0.0498	0.0011	112.0466	$C_T > 0$	K+pi-
K*0(892)	0.8939	0.0005	0.0478	0.0010	94.4253	$C_T < 0$	

Figure 23: The fitted values from the curves in Fig.24,25,26(MeV)

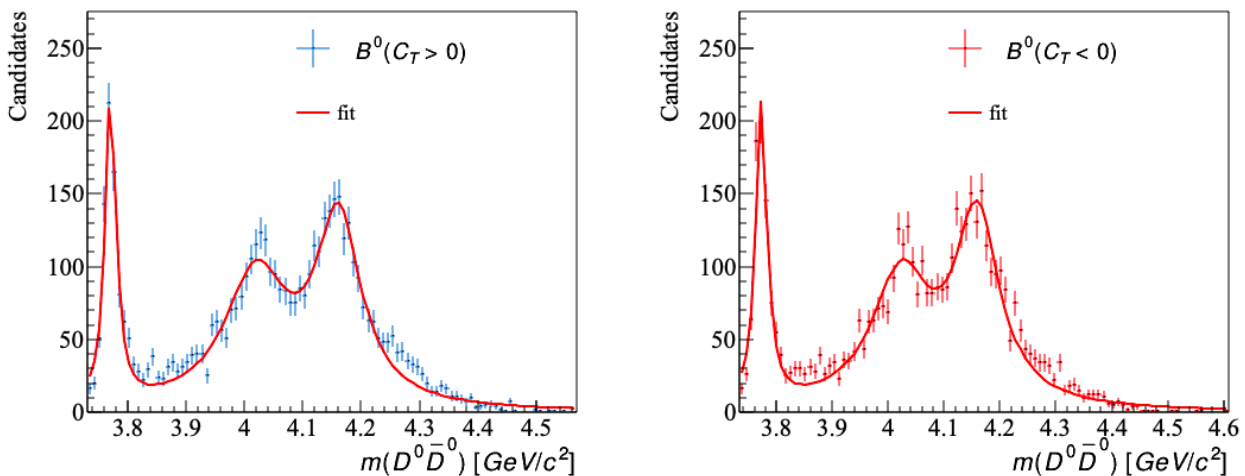


Figure 24: The binned distributions of invariant mass $m(D^0\bar{D}^0)$ for different values of C_T .

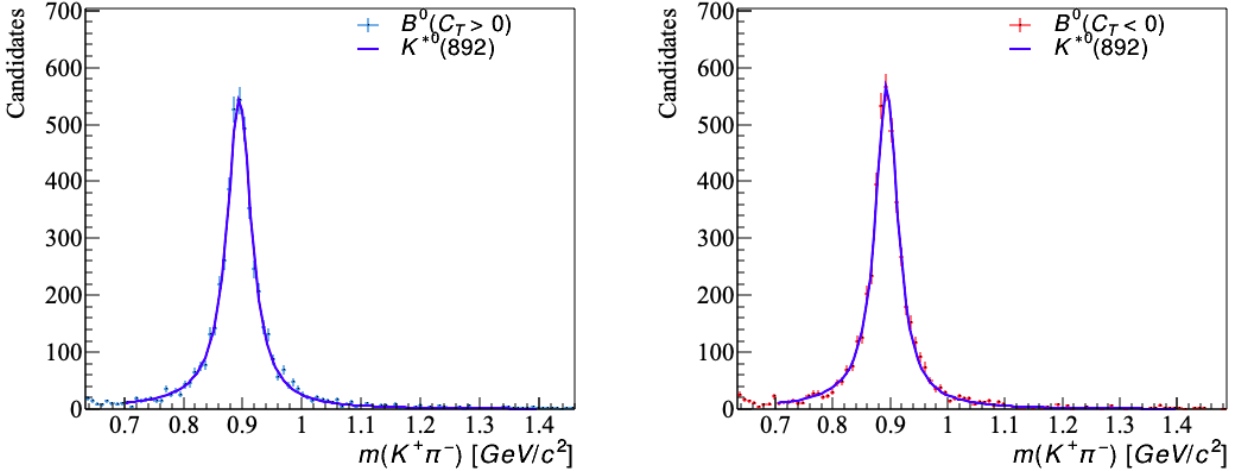


Figure 25: The binned distributions of invariant mass $m(K^+\pi^-)$ for different values of C_T .

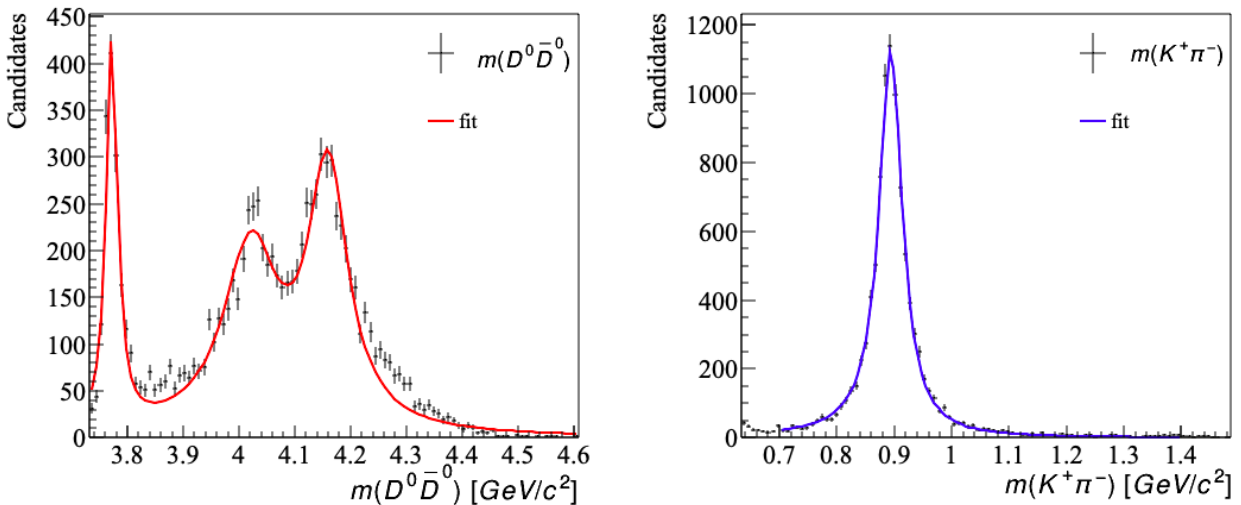


Figure 26: The binned distributions of invariant mass $m(D^0\bar{D}^0)$ for different values of C_T .

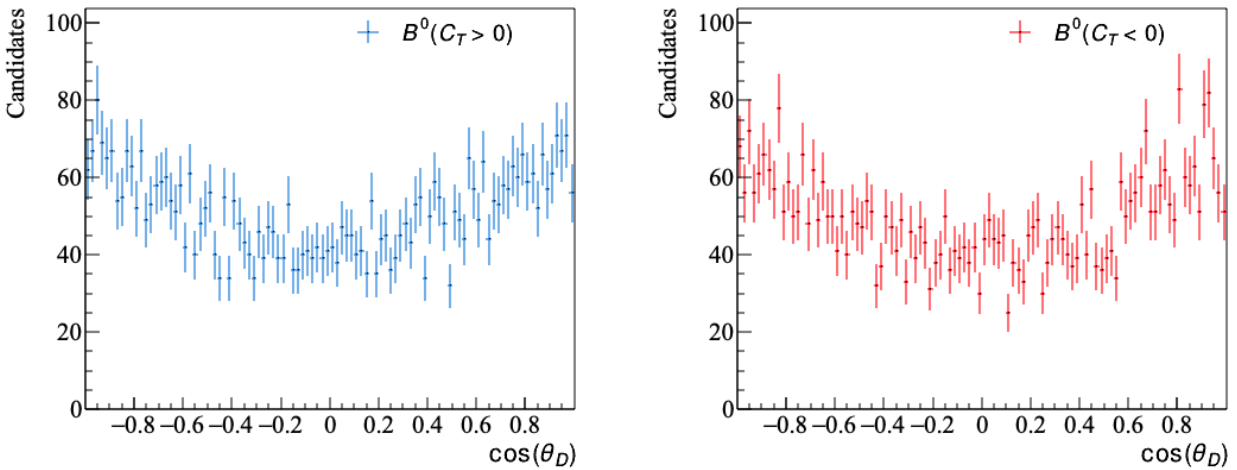


Figure 27: The binned distributions of helicity angle $\cos(\theta_{D^0})$ for different values of C_T .

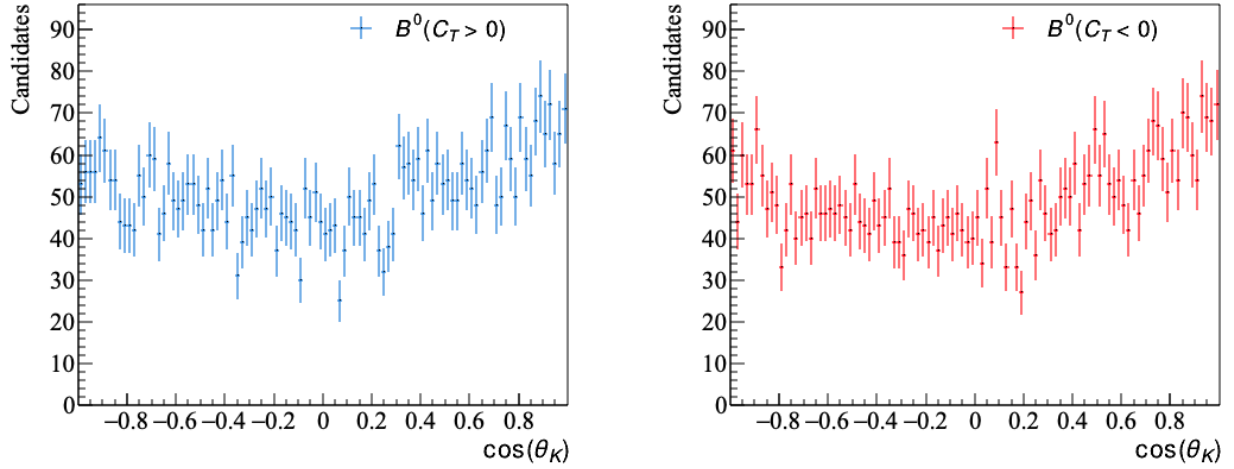


Figure 28: The binned distributions of helicity angle $\cos(\theta_{K+})$ for different values of C_T .

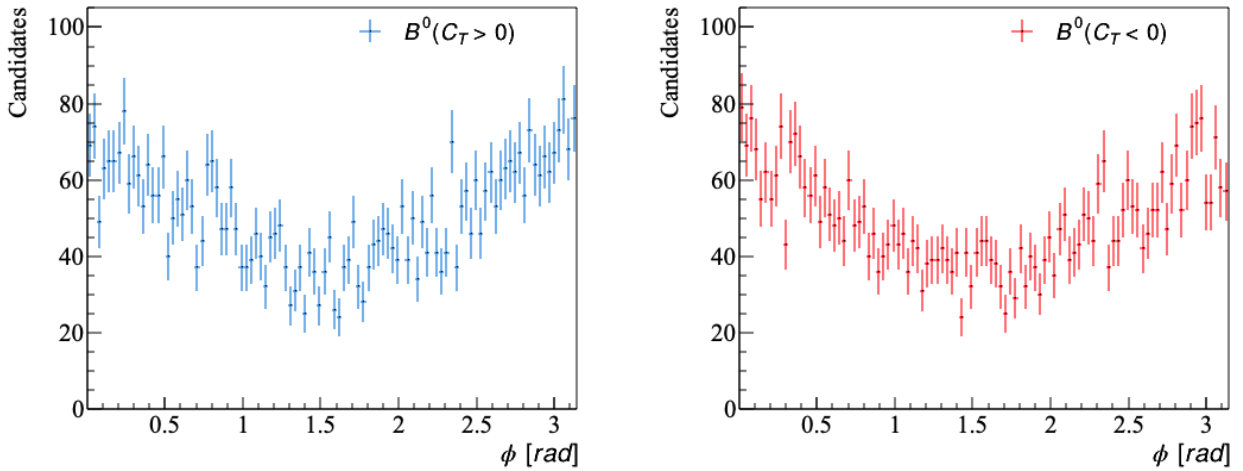


Figure 29: The binned distributions of the angle ϕ between the plane $D^0\bar{D}^0$ and the plane $K^+\pi^-$ for different values of C_T .

To do list:

- CP violation for D0 and for B0 decay.
- split spins, 1/3 amplitude and make the phase equal
- check the amount of CP violation vs number of events
- check p violation in several decay modes
- check K~, pi# meaning in the root file (try flipping the sign of the momentum for _3_K~ and _4_pi#)
⇒ have got the same results for CM variables

The charge conjugate decays can be generated using a different Seed in AmpGen (e.g. add a line in the .opt file: Seed 6) and filpping the sign in the three momentum and adding a minus sign before \bar{C}_T .

a. Find the CP violation in $D^0 \rightarrow K^+ K^- \pi^+ \pi^-$ decay:

Re-run the DtoKKpipi_v2.opt file using Seed 5, gives

$$\begin{aligned} \bar{A}_T &= -0.072563 \pm 0.0024, \text{ and together with} \\ A_T &= -0.073987 \pm 0.0024 \text{ (previous results),} \\ \text{gives } \mathcal{A}_{CP} &= 0.5(A_T - \bar{A}_T) = -0.000712 \pm 0.0017. \end{aligned}$$

This is over a half smaller than the literature.

b. Find the CP violation in $B^0 \rightarrow D^0 \bar{D}^0 K^+ \pi^-$ decay:

Re-run the B0toDDbar0K+pi-.opt file twice after adding NonResS0, with 10000 events, using Seed 5 and 7, gives

$$\begin{aligned} A_T &= 0.012 \pm 0.00999927, \\ \bar{A}_T &= 0.0102 \pm 0.00999947, \\ \text{and, hence } \mathcal{A}_{CP} &= 0.5(A_T - \bar{A}_T) = 0.000899999999999998 \pm 0.007070622334946903. \end{aligned}$$

For 100000 events, with the B0 decay, no seed specified (seed 0), gives

$$A_T = 0.0014978601997146933 \pm 0.003447862046481769,$$

conjugate process using Seed 8 gives,

$$\bar{A}_T = -0.00148 \pm 0.0031622741968399893,$$

find $\mathcal{A}_{CP} = 0.001488930099857346 \pm 0.002339216256974195$.

This value of \mathcal{A}_{CP} was investigated further for a range of event numbers:

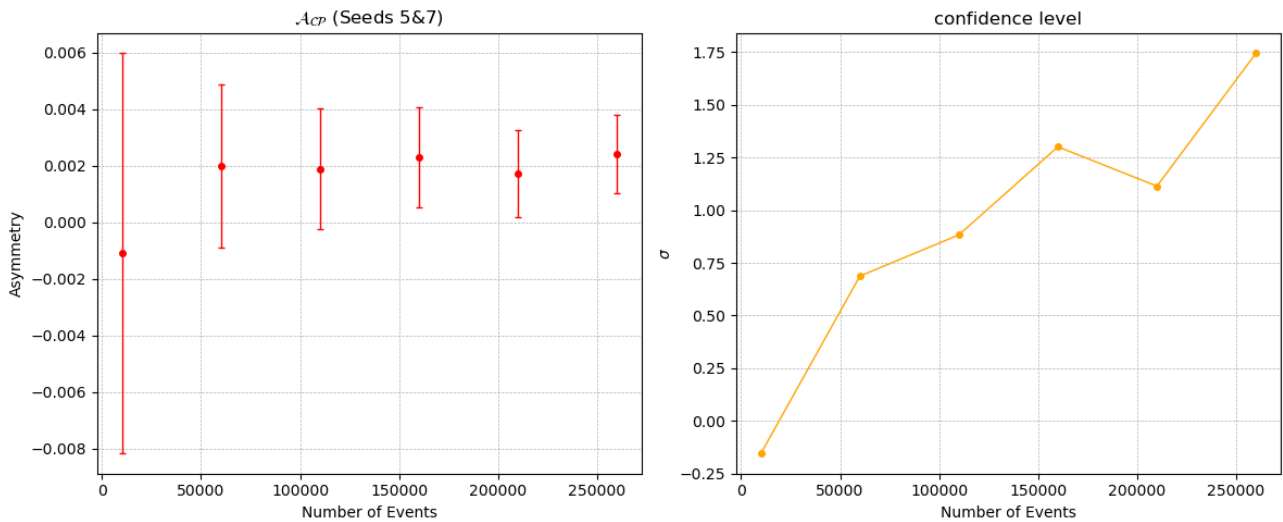


Figure 30: The asymmetries calculated for different number of events.

It can be seen that the a_{CP} is slightly deviated from zero with errorbars becoming smaller and excluding zero, but the confidence level is less than 2σ , where $\sigma = \text{asymmetry}/\Delta(\text{asymmetry})$. Clearly, more events need to be generated to see the trend of asymmetry and error bars.

13 Feb 2020, Thursday

Generate the S, P, D waves for two spin-1 particles

From Paras:

One is that we indeed still have to specify independent couplings of differing spin configurations separately. In practical terms, for the "vector-vector" decays i.e decays to two spin-1 particles (such as $B-\zeta\psi K^*$) we need to specify S P and D waves, there should be examples of this in the $D-\zeta KK\pi\pi$ opt file. We should discuss at some point how to split the amplitude and phase across the components (first instinct: make each amplitude 1/3 of the current value, and make all phases the same)

So in the $B0\text{to}DDbar0K+\pi\text{-v3}.opt$ file, the two spin-1 particles are:

$\psi(3770)$ and $K^*(892)0$
 $\psi(4040)$ and $K^*(892)0$
 $\psi(4160)$ and $K^*(892)0$
 $\psi(4415)$ and $K^*(892)0$

The changes made are e.g

For a single resonance,

$B0\{\psi(3770)0\{D0,Dbar0\},K^*(892)0\{K^+,\pi^-\}\} \quad 2 \quad 6.28 \quad 0.05 \quad 2 \quad 0. \quad 10.$

This was changed by taking 1/3 of the second number column - amplitude):

$B0[S]\{\psi(3770)0\{D0,Dbar0\},K^*(892)0\{K^+,\pi^-\}\} \quad 2 \quad 2.093 \quad 0.05 \quad 2 \quad 0. \quad 10.$
 $B0[P]\{\psi(3770)0\{D0,Dbar0\},K^*(892)0\{K^+,\pi^-\}\} \quad 2 \quad 2.093 \quad 0.05 \quad 2 \quad 0. \quad 10.$
 $B0[D]\{\psi(3770)0\{D0,Dbar0\},K^*(892)0\{K^+,\pi^-\}\} \quad 2 \quad 2.093 \quad 0.05 \quad 2 \quad 0. \quad 10.$

- There are no errors generated and gives different values in the output file.

Next:

Adjust the p waves and check p-violation
test for more event numbers
use different seeds

The events were generated with increasing event numbers and smaller intervals. It can be seen in Fig.31 that there is a fluctuation in the asymmetries at around $2 \cdot 10^5$ events and the asymmetries goes to zero at larger events numbers. This shows no CP and P violation. The errors in the asymmetries decreases asymptotically closing to zero as the event number increases.

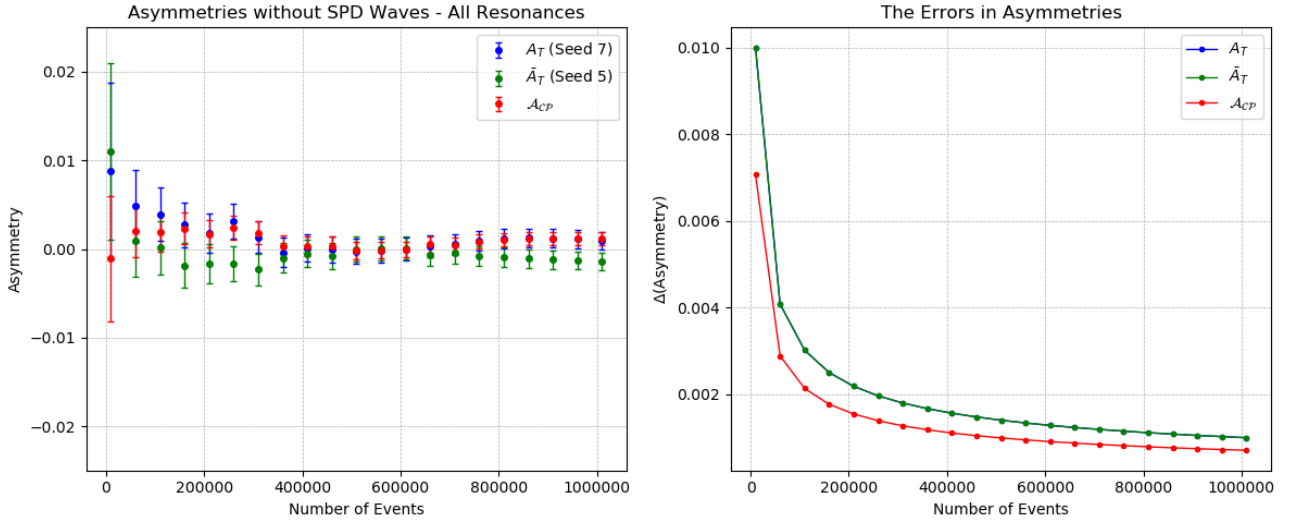


Figure 31: The asymmetries calculated for different number of events.

With the SPD waves, as shown in Fig.32, the values of A_T and \bar{A}_T are no longer consistent with zero which means there are P violation induced in both decay processes.

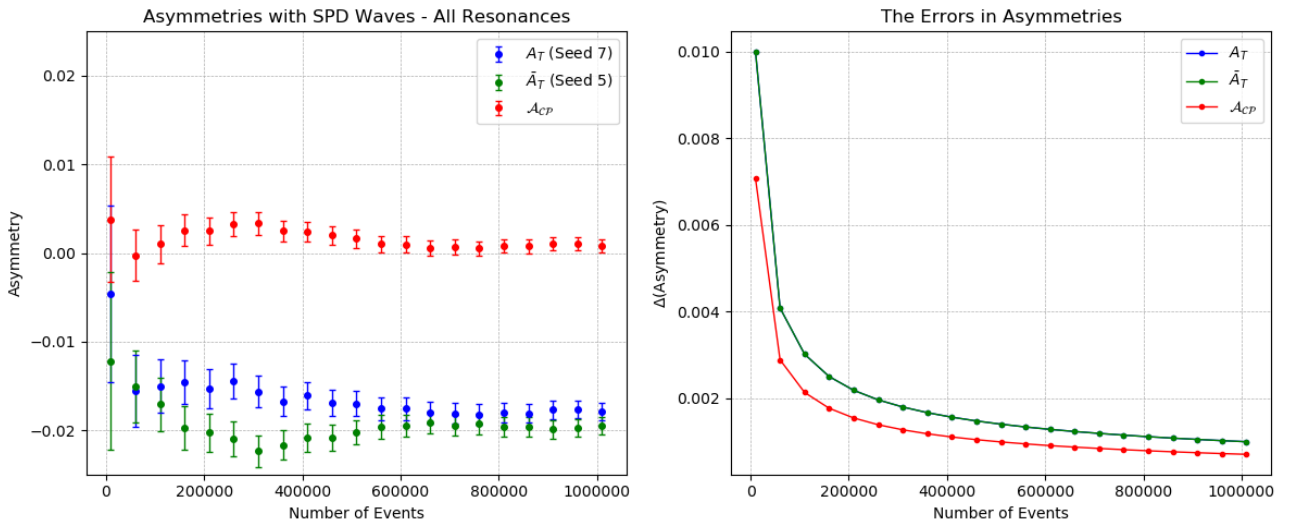


Figure 32: The asymmetries calculated for different number of events with equal SPD waves.

This part starts by changing P waves in the resonance files:

A. Change all P wave amplitudes

Input files: AmpGen/build/bin/spd_waves_gen

Output files: Simulations/B02DDbarKPi/p_waves

event file (.opt) Example:

```

1 EventType B0 D0 Dbar0 K+ pi-
2
3 B0{NonResS0{D0,Dbar0},K*(892)0{K+,pi-}} 0    2.09    1.  0  0  10
4
5 B0{NonResS0{D0,Dbar0},K(0)*(1430)0{K+,pi-}} 0    0.66    1.  0  0  10
6
7 B0{K(0)*(800)0{K+,pi-},NonResS0{D0,Dbar0}} 0    0.66    1.  0  0  10
8
9 B0{D(s2)(2573)+{D0,K+},Dbar0,pi-} 0      0.10   0.05 0      0.     10.
10
11 B0[S]{psi(3770)0{D0,Dbar0},K*(892)0{K+,pi-}} 2      2.093  0.05  2   0.  10.
12 B0[P]{psi(3770)0{D0,Dbar0},K*(892)0{K+,pi-}} 2      0.002093 0.05  2   0.  10.
13 B0[D]{psi(3770)0{D0,Dbar0},K*(892)0{K+,pi-}} 2      2.093  0.05  2   0.  10.
14
15 B0[P]{psi(4040)0{D0,Dbar0},K*(892)0{K+,pi-}} 0      0.000826 0.05  0   0.  10.
16 B0[S]{psi(4040)0{D0,Dbar0},K*(892)0{K+,pi-}} 0      0.826   0.05  0   0.  10.
17 B0[D]{psi(4040)0{D0,Dbar0},K*(892)0{K+,pi-}} 0      0.826   0.05  0   0.  10.
18
19 B0[D]{psi(4160)0{D0,Dbar0},K*(892)0{K+,pi-}} 0      1.31    0.05  0.  0.  10.
20 B0[S]{psi(4160)0{D0,Dbar0},K*(892)0{K+,pi-}} 0      1.31    0.05  0.  0.  10.
21 B0[P]{psi(4160)0{D0,Dbar0},K*(892)0{K+,pi-}} 0      0.00131 0.05  0.  0.  10.
22
23 B0[P]{psi(4415)0{D0,Dbar0},K*(892)0{K+,pi-}} 0      0.00051 0.05  0.  0.  10.
24 B0[S]{psi(4415)0{D0,Dbar0},K*(892)0{K+,pi-}} 0      0.51    0.05  0.  0.  10.
25 B0[D]{psi(4415)0{D0,Dbar0},K*(892)0{K+,pi-}} 0      0.51    0.05  0.  0.  10.
26
27 B0{psi(3770)0{D0,Dbar0},K(0)*(800)0{K+,pi-}} 0      1.99    0.05  0.  0.  10.
28 B0{psi(4040)0{D0,Dbar0},K(0)*(800)0{K+,pi-}} 0      0.78    0.05  0.  0.  10.
29 B0{psi(4160)0{D0,Dbar0},K(0)*(800)0{K+,pi-}} 0      1.24    0.05  0.  0.  10.
30 B0{psi(4415)0{D0,Dbar0},K(0)*(800)0{K+,pi-}} 0      0.48    0.05  0.  0.  10.
31
32 B0{psi(3770)0{D0,Dbar0},K(0)*(1430)0{K+,pi-}} 0      1.99    0.05  0.  0.  10.
33 B0{psi(4040)0{D0,Dbar0},K(0)*(1430)0{K+,pi-}} 0      0.78    0.05  0.  0.  10.
34 B0{psi(4160)0{D0,Dbar0},K(0)*(1430)0{K+,pi-}} 0      1.24    0.05  0.  0.  10.
35 B0{psi(4415)0{D0,Dbar0},K(0)*(1430)0{K+,pi-}} 0      0.48    0.05  0.  0.  10.
36
37 #B0{Z(c)(3900)+{D*(2010)+{D0,pi+},Dbar0},K-} 2   1   0   2   0   0

```

Figure 33: An example of event file for the plot in Fig.36

Changed the second number column in line 12, 15, 21, 23.

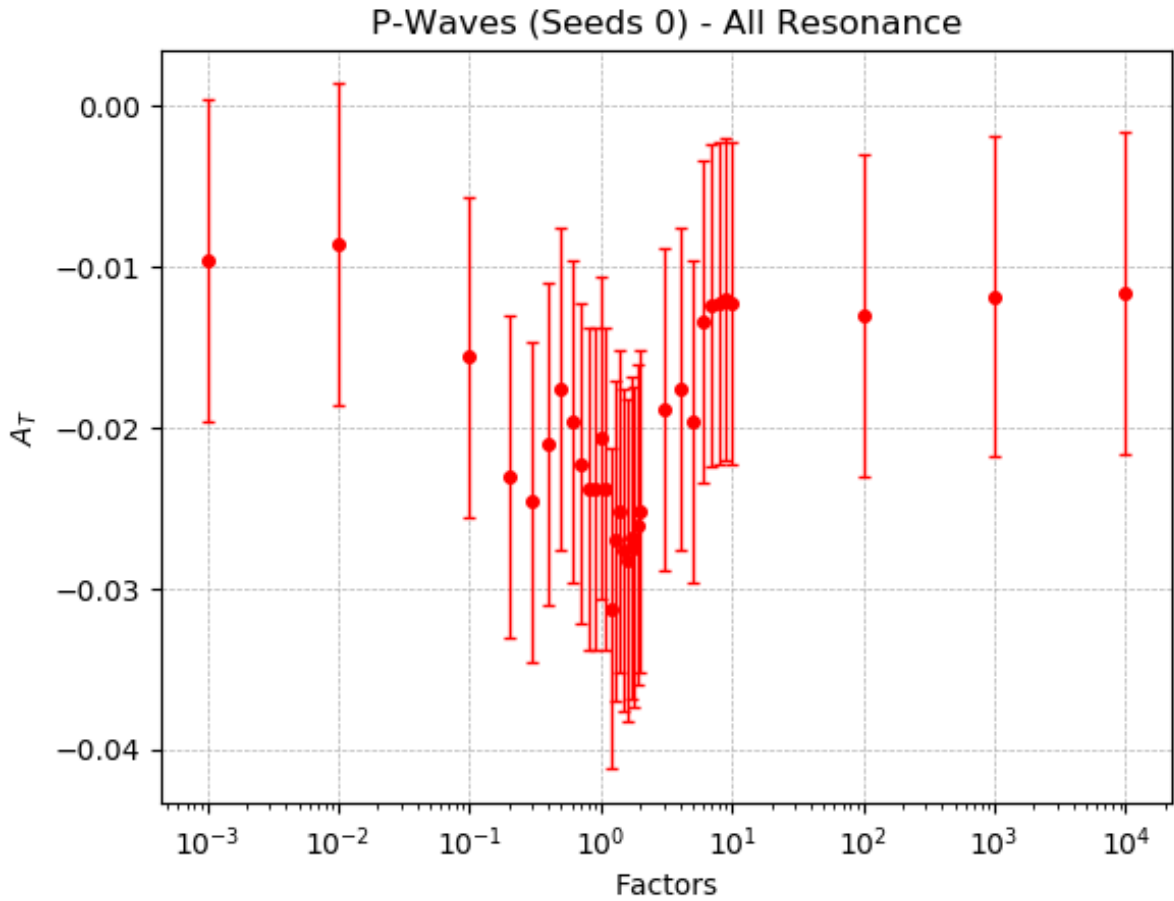


Figure 34: The change of A_T by multiplying all the P wave amplitudes with the factors in x-axis using 10^4 events.

All the events and P wave values are generated with the same seed - no seed specified (Seed 0).

B. Change all SP wave amplitudes and make them equal

Input files: AmpGen/build/bin/spd_waves_gen

Output files: Simulations/B02DDbarKPi/sp_waves

event file (.opt) Example:

```

1 EventType B0 D0 Dbar0 K+ pi-
2
3 B0{NonResS0{D0,Dbar0},K*(892)0{K+,pi-}} 0    2.09    1.  0   0   10
4
5 B0{NonResS0{D0,Dbar0},K(0)*(1430)0{K+,pi-}} 0    0.66    1.  0   0   10
6
7 B0{K(0)*(800)0{K+,pi-},NonResS0{D0,Dbar0}} 0    0.66    1.  0   0   10
8
9 B0{D(s2)(2573)+{D0,K+},Dbar0,pi-} 0      0.10    0.05 0      0.      10.
10
11 B0[S]{psi(3770)0{D0,Dbar0},K*(892)0{K+,pi-}} 2      0.002093  0.05    2  0.  10.
12 B0[P]{psi(3770)0{D0,Dbar0},K*(892)0{K+,pi-}} 2      0.002093  0.05    2  0.  10.
13 B0[D]{psi(3770)0{D0,Dbar0},K*(892)0{K+,pi-}} 2      2.093   0.05    2  0.  10.
14
15 B0[P]{psi(4040)0{D0,Dbar0},K*(892)0{K+,pi-}} 0      0.000826  0.05    0  0.  10.
16 B0[S]{psi(4040)0{D0,Dbar0},K*(892)0{K+,pi-}} 0      0.000826  0.05    0  0.  10.
17 B0[D]{psi(4040)0{D0,Dbar0},K*(892)0{K+,pi-}} 0      0.826    0.05    0  0.  10.
18
19 B0[D]{psi(4160)0{D0,Dbar0},K*(892)0{K+,pi-}} 0      1.31    0.05    0.  0.  10.
20 B0[S]{psi(4160)0{D0,Dbar0},K*(892)0{K+,pi-}} 0      0.00131  0.05    0.  0.  10.
21 B0[P]{psi(4160)0{D0,Dbar0},K*(892)0{K+,pi-}} 0      0.00131  0.05    0.  0.  10.
22
23 B0[P]{psi(4415)0{D0,Dbar0},K*(892)0{K+,pi-}} 0      0.00051  0.05    0.  0.  10.
24 B0[S]{psi(4415)0{D0,Dbar0},K*(892)0{K+,pi-}} 0      0.00051  0.05    0.  0.  10.
25 B0[D]{psi(4415)0{D0,Dbar0},K*(892)0{K+,pi-}} 0      0.51    0.05    0.  0.  10.
26
27 B0{psi(3770)0{D0,Dbar0},K(0)*(800)0{K+,pi-}} 0      1.99    0.05    0.  0.  10.
28 B0{psi(4040)0{D0,Dbar0},K(0)*(800)0{K+,pi-}} 0      0.78    0.05    0.  0.  10.
29 B0{psi(4160)0{D0,Dbar0},K(0)*(800)0{K+,pi-}} 0      1.24    0.05    0.  0.  10.
30 B0{psi(4415)0{D0,Dbar0},K(0)*(800)0{K+,pi-}} 0      0.48    0.05    0.  0.  10.
31
32 B0{psi(3770)0{D0,Dbar0},K(0)*(1430)0{K+,pi-}} 0      1.99    0.05    0.  0.  10.
33 B0{psi(4040)0{D0,Dbar0},K(0)*(1430)0{K+,pi-}} 0      0.78    0.05    0.  0.  10.
34 B0{psi(4160)0{D0,Dbar0},K(0)*(1430)0{K+,pi-}} 0      1.24    0.05    0.  0.  10.
35 B0{psi(4415)0{D0,Dbar0},K(0)*(1430)0{K+,pi-}} 0      0.48    0.05    0.  0.  10.
36
37 #B0{Z(c)(3900)+{D*(2010)+{D0,pi+},Dbar0},K-} 2  1  0  2  0  0

```

Figure 35: An example of event file for the plot in Fig.36

Changed the second number column in line 11, 12, 15, 16, 20, 21, 23, 24.

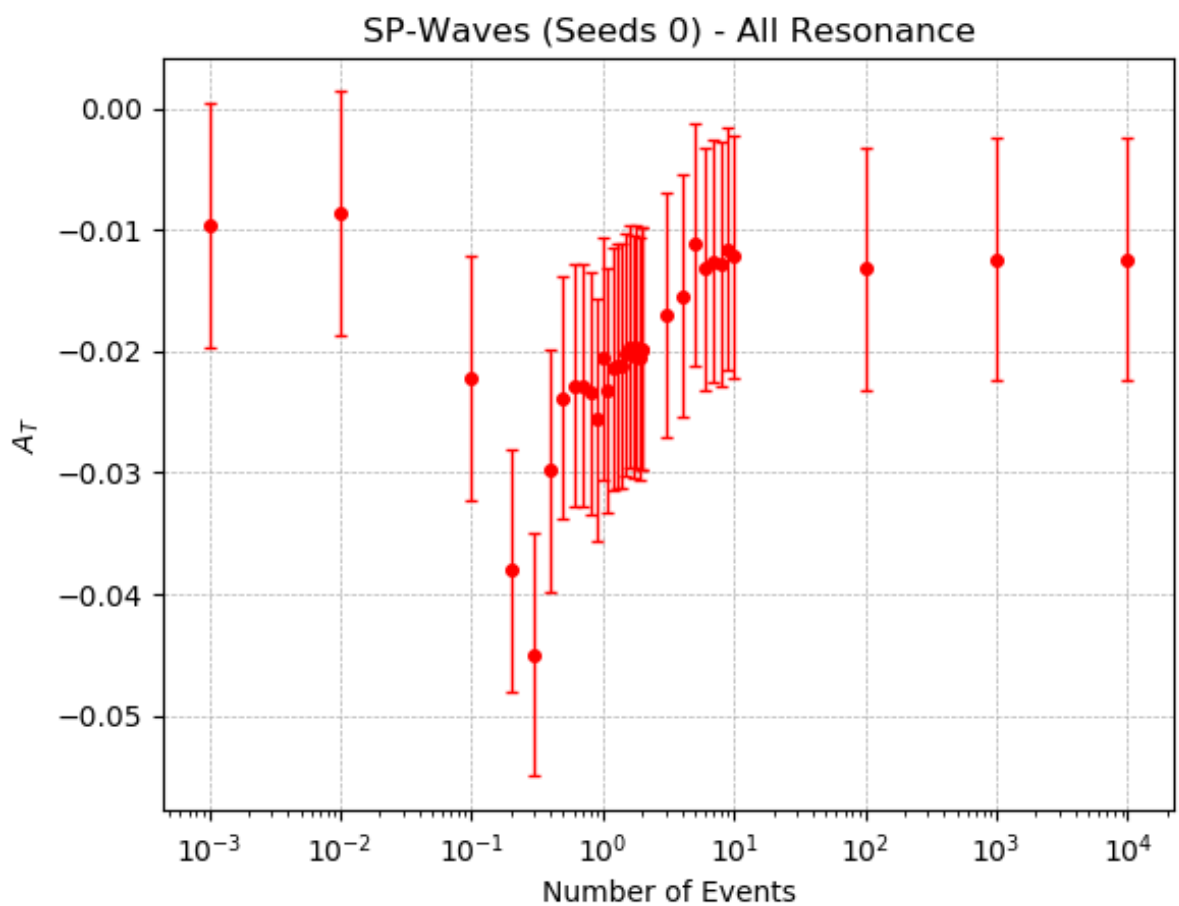


Figure 36: The change of A_T by multiplying all the S and P wave amplitudes with the factors in x-axis using 10^4 events.

C. P waves and SP waves for all resonances

Input files: AmpGen/build/bin/spd_waves_gen_sr2

Output files: Simulations/B02DDbarKPi/spd_waves_sr2

event file (.opt) Example:

```

~/AmpGen/build/bin/spd_waves_gen_sr2/B0toDDbar0K+pi-_p1E-3.opt
1 EventType B0 D0 Dbar0 K+ pi-
2
3 B0{NonResS0{D0,Dbar0},K*(892)0{K+,pi-}} 0    2.09    1.  0  0  10
4
5 B0{NonResS0{D0,Dbar0},K(0)*(1430)0{K+,pi-}} 0    0.66    1.  0  0  10
6
7 B0{K(0)*(800)0{K+,pi-},NonResS0{D0,Dbar0}} 0    0.66    1.  0  0  10
8
9 B0{D(s2)(2573)+{D0,K+},Dbar0,pi-} 0    0.10    0.05 0    0.    10.
10
11 B0[P]{psi(3770)0{D0,Dbar0},K*(892)0{K+,pi-}} 2    0.002093  0.05  2  0.  10.
12
13 B0[P]{psi(4040)0{D0,Dbar0},K*(892)0{K+,pi-}} 0    0.000826  0.05  0    0.  10.
14
15 B0[P]{psi(4160)0{D0,Dbar0},K*(892)0{K+,pi-}} 0    0.00131  0.05  0.  0.  10.
16
17 B0[P]{psi(4415)0{D0,Dbar0},K*(892)0{K+,pi-}} 0    0.00051  0.05  0.  0.  10.
18
19 B0{psi(3770)0{D0,Dbar0},K(0)*(800)0{K+,pi-}} 0    1.99    0.05  0.  0.  10.
20
21 B0{psi(4040)0{D0,Dbar0},K(0)*(800)0{K+,pi-}} 0    0.78    0.05  0.  0.  10.
22
23 B0{psi(4160)0{D0,Dbar0},K(0)*(800)0{K+,pi-}} 0    1.24    0.05  0.  0.  10.
24
25 B0{psi(4415)0{D0,Dbar0},K(0)*(800)0{K+,pi-}} 0    0.48    0.05  0.  0.  10.
26
27 B0{psi(3770)0{D0,Dbar0},K(0)*(1430)0{K+,pi-}} 0    1.99    0.05  0.  0.  10.
28
29 B0{psi(4040)0{D0,Dbar0},K(0)*(1430)0{K+,pi-}} 0    0.78    0.05  0.  0.  10.
30
31 B0{psi(4160)0{D0,Dbar0},K(0)*(1430)0{K+,pi-}} 0    1.24    0.05  0.  0.  10.
32
33 B0{psi(4415)0{D0,Dbar0},K(0)*(1430)0{K+,pi-}} 0    0.48    0.05  0.  0.  10.
34
35 #B0{Z(c)(3900)+{D*(2010)+{D0,pi+},Dbar0},K-} 2  1  0  2  0  0

```

Figure 37: An example of event file for the P-wave plot in Fig.39

Changed the second number column in line 11, 13, 15, 17.

Changed the second number column in line 11, 12, 14, 15, 17, 18, 20, 21.

```
~/AmpGen/build/bin/spd_waves_gen_sr2/B0toDDbar0K+pi-_sp1E-3.opt -
```

```

1 EventType B0 D0 Dbar0 K+ pi-
2
3 B0{NonResS0{D0,Dbar0},K*(892)0{K+,pi-}} 0 2.09 1. 0 0 10
4
5 B0{NonResS0{D0,Dbar0},K(0)*(1430)0{K+,pi-}} 0 0.66 1. 0 0 10
6
7 B0{K(0)*(800)0{K+,pi-},NonResS0{D0,Dbar0}} 0 0.66 1. 0 0 10
8
9 B0{D(s2)(2573)+{D0,K+},Dbar0,pi-} 0 0.10 0.05 0 0. 10.
10
11 B0[P]{psi(3770)0{D0,Dbar0},K*(892)0{K+,pi-}} 2 0.002093 0.05 2 0. 10.
12 B0[S]{psi(3770)0{D0,Dbar0},K*(892)0{K+,pi-}} 2 0.002093 0.05 2 0. 10.
13
14 B0[P]{psi(4040)0{D0,Dbar0},K*(892)0{K+,pi-}} 0 0.000826 0.05 0 0. 10.
15 B0[S]{psi(4040)0{D0,Dbar0},K*(892)0{K+,pi-}} 0 0.000826 0.05 0 0. 10.
16
17 B0[P]{psi(4160)0{D0,Dbar0},K*(892)0{K+,pi-}} 0 0.00131 0.05 0. 0. 10.
18 B0[S]{psi(4160)0{D0,Dbar0},K*(892)0{K+,pi-}} 0 0.00131 0.05 0. 0. 10.
19
20 B0[P]{psi(4415)0{D0,Dbar0},K*(892)0{K+,pi-}} 0 0.00051 0.05 0. 0. 10.
21 B0[S]{psi(4415)0{D0,Dbar0},K*(892)0{K+,pi-}} 0 0.00051 0.05 0. 0. 10.
22
23 B0{psi(3770)0{D0,Dbar0},K(0)*(800)0{K+,pi-}} 0 1.99 0.05 0. 0. 10.
24
25 B0{psi(4040)0{D0,Dbar0},K(0)*(800)0{K+,pi-}} 0 0.78 0.05 0. 0. 10.
26
27 B0{psi(4160)0{D0,Dbar0},K(0)*(800)0{K+,pi-}} 0 1.24 0.05 0. 0. 10.
28
29 B0{psi(4415)0{D0,Dbar0},K(0)*(800)0{K+,pi-}} 0 0.48 0.05 0. 0. 10.
30
31 B0{psi(3770)0{D0,Dbar0},K(0)*(1430)0{K+,pi-}} 0 1.99 0.05 0. 0. 10.
32
33 B0{psi(4040)0{D0,Dbar0},K(0)*(1430)0{K+,pi-}} 0 0.78 0.05 0. 0. 10.
34
35 B0{psi(4160)0{D0,Dbar0},K(0)*(1430)0{K+,pi-}} 0 1.24 0.05 0. 0. 10.
36
37 B0{psi(4415)0{D0,Dbar0},K(0)*(1430)0{K+,pi-}} 0 0.48 0.05 0. 0. 10.
38
39 #B0{Z(c)(3900)+{D*(2010)+{D0,pi+},Dbar0},K-} 2 1 0 2 0 0
40

```

Figure 38: An example of event file for the SP-wave plot in Fig.39

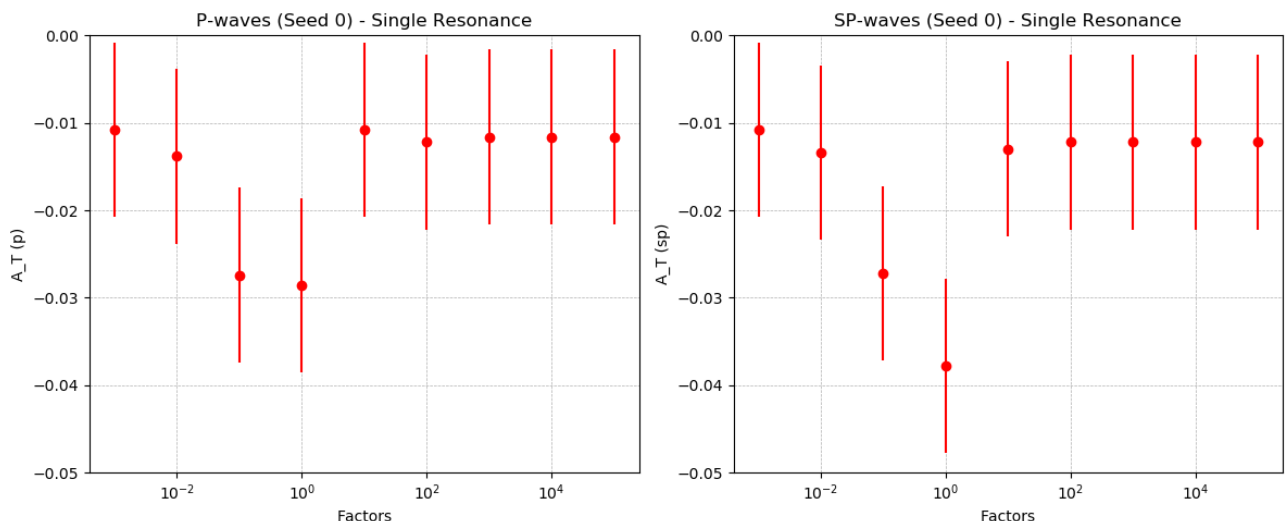


Figure 39: (left) The change of A_T by multiplying the P wave amplitudes with the factors in x-axis using 10^4 events. (right) The change of A_T by multiplying the S and P wave amplitudes equally with the factors in x-axis using 10^4 events.

Investigation on single resonance $\psi(3770)\text{K}^*(892)0$:

D. use only the P waves or SP waves for a single resonance

Input files: AmpGen/build/bin/spd_waves_gen_sr1

Output files: Simulations/B02DDbarKPi/spd_waves_sr1

event file (.opt) Example:

```
~/AmpGen/build/bin/spd_waves_gen_sr1/B0toDDbar0K+pi-_p1E-3.opt
1 EventType B0 D0 Dbar0 K+ pi-
2
3 B0[P]{psi(3770)0{D0,Dbar0},K*(892)0{K+,pi-}} 2 0.002093 0.05 2 0. 10.
```

Figure 40: An example of event file for the P-wave plot in Fig.42

Changed the second number column in line 3.

```
~/AmpGen/build/bin/spd_waves_gen_sr1/B0toDDbar0K+pi-_sp1E-3.opt
1 EventType B0 D0 Dbar0 K+ pi-
2
3
4
5 B0[S]{psi(3770)0{D0,Dbar0},K*(892)0{K+,pi-}} 2 0.002093 0.05 2 0. 10.
6 B0[P]{psi(3770)0{D0,Dbar0},K*(892)0{K+,pi-}} 2 0.002093 0.05 2 0. 10.
```

Figure 41: An example of event file for the SP-wave plot in Fig.42

Changed the second number column in line 5, 6. Reasons for flat?

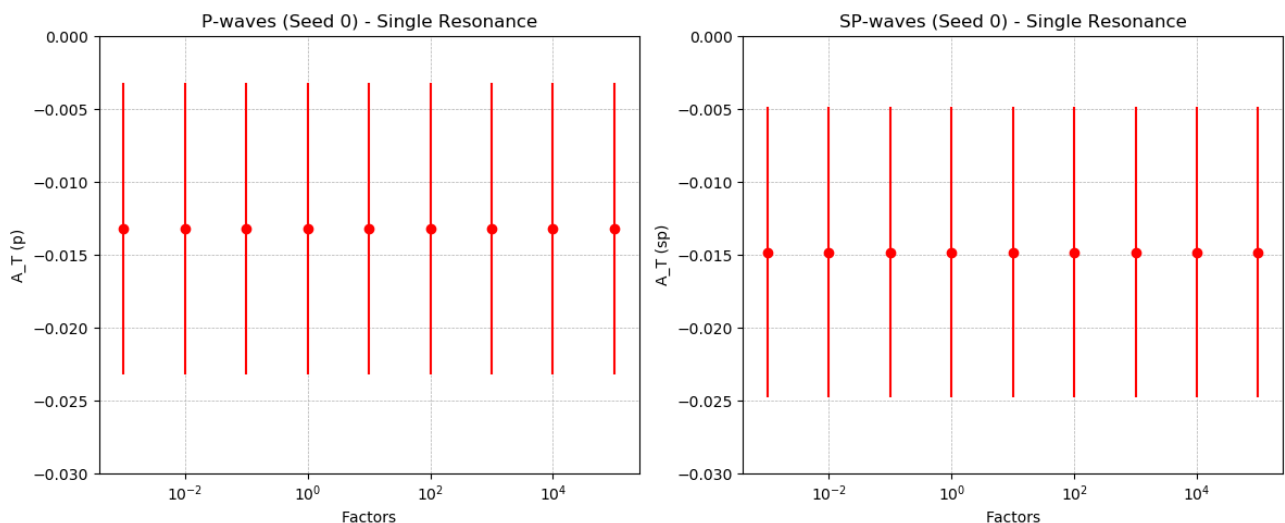


Figure 42: (left) The change of A_T by multiplying the P wave amplitudes with the factors in x-axis using 10^4 events. (right) The change of A_T by multiplying the S and P wave amplitudes equally with the factors in x-axis using 10^4 events.

Investigation on single resonance $\psi(4040)K^*(892)0$: E. P waves and SP waves single resonances with interferences

Input files: AmpGen/build/bin/spd_waves_gen_sr3
 AmpGen/build/bin/B0_event_spd_sr3_4040/sr1_seed200_10000 (for smaller intervals between -1 and 1)

Output files: Simulations/B02DDbarKPi/spd_waves_sr3
 Simulations/B02DDbarKPi/spd_waves_sr_4040

event file (.opt) Example:

```
~/AmpGen/build/bin/spd_waves_gen_sr3/B0toDDbar0K+pi-_p1E-3.opt +
1 EventType B0 D0 Dbar0 K+ pi-
2
3 B0[P]{psi(4040)0{D0,Dbar0},K*(892)0{K+,pi-}} 0 0.000826 0.05 0 0. 10.
4 B0[S]{psi(4040)0{D0,Dbar0},K*(892)0{K+,pi-}} 0 0.826 0.05 0 0. 10.
5
```

Figure 43: An example of event file for the P-wave plot in Fig.45

Changed the second number column in line 3.

```
~/AmpGen/build/bin/spd_waves_gen_sr3/B0toDDbar0K+pi-_sp1E-3.opt +
1 EventType B0 D0 Dbar0 K+ pi-
2
3 B0[P]{psi(4040)0{D0,Dbar0},K*(892)0{K+,pi-}} 0 0.000826 0.05 0 0. 10.
4 B0[S]{psi(4040)0{D0,Dbar0},K*(892)0{K+,pi-}} 0 0.000826 0.05 0 0. 10.
5 B0[D]{psi(4040)0{D0,Dbar0},K*(892)0{K+,pi-}} 0 0.826 0.05 0 0. 10.
```

Figure 44: An example of event file for the SP-wave plot in Fig.45

Changed the second number column in line 3, 4.

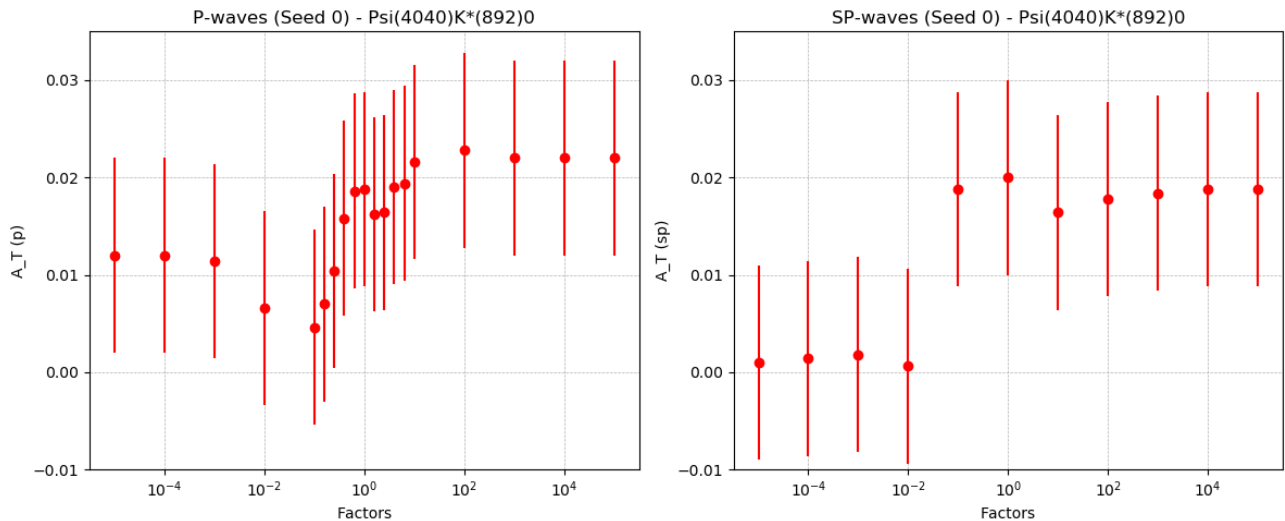


Figure 45: (left) The change of A_T by multiplying the P wave amplitudes with the factors in x-axis using 10^4 events. (right) The change of A_T by multiplying the S and P wave amplitudes equally with the factors in x-axis using 10^4 events.

21 Feb 2020, Friday

F. Split the events into ten files generated with a set of 10 seeds

(1) Same set of seed for each p wave amplitude:

Seed 0,10,20,30,40,50,60,70,80,90 — range (0,100,10)

Input files: AmpGen/build/bin/spd_waves_gen_sr3_seed

AmpGen/build/bin/B0_event_spd_sr3_4040/sr2_seed200_1000 (for smaller intervals between -1 and 1)

Output files: Simulations/B02DDbarKPi/spd_waves_combine_1E4_4040

Simulations/B02DDbarKPi/spd_waves_sr_4040

event file (.opt) Example:

```
~/AmpGen/build/bin/spd_waves_gen_sr3_seed/B0toDDbar0K+pi-_p1E-1_s20.opt
1 EventType B0 D0 Dbar0 K+ pi-
2
3 B0[P]{psi(4040)0{D0,Dbar0},K*(892)0{K+,pi-}} 0 0.0826 0.05 0 0. 10.
4 B0[S]{psi(4040)0{D0,Dbar0},K*(892)0{K+,pi-}} 0 0.826 0.05 0 0. 10.
5
6 Seed 20
```

Figure 46: An example of event file for the P-wave plot in Fig.47

Changed the second number column in line 3, 6.

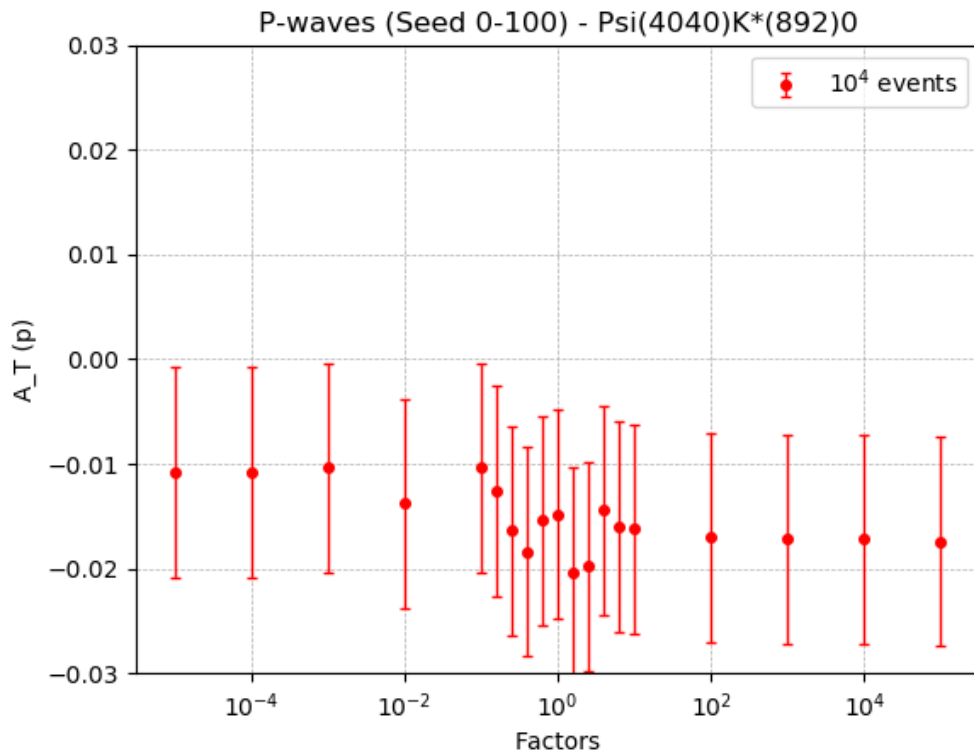


Figure 47: The change of A_T by multiplying the P wave amplitudes with the factors in x-axis using 10^4 events.

(2) Different sets of seed for each p wave amplitude:

e.g - Seed 0,20,40,60,80,100,120,140,160,180 — range (0,200,10) for $factor = 10^{-5}$

Seed 1,21,41,61,81,101,121,141,161,181 for $factor = 10^{-4}$

, etc...

Input files: AmpGen/build/bin/spd_waves_gen_sr3_seed2

AmpGen/build/bin/B0_event_spd_sr3_4040/sr3_seed200_1000 + sr3_seed200_10000 (for smaller intervals between -1 and 1)

Output files: Simulations/B02DDbarKPi/spd_waves_combined2_1E4_4040 + spd_waves_combined2_1E5_4040

Simulations/B02DDbarKPi/spd_waves_sr_4040

event file (.opt) Example:

```
~/AmpGen/build/bin/spd_waves_gen_sr3_seed2/output_opt_1E4/B0toDDbar0K+pi-_p1E-1_s64.opt
1 EventType B0 D0 Dbar0 K+ pi-
2
3 B0[P]{psi(4040)0{D0,Dbar0},K*(892)0{K+,pi-}} 0 0.0826 0.05 0 0. 10.
4 B0[S]{psi(4040)0{D0,Dbar0},K*(892)0{K+,pi-}} 0 0.826 0.05 0 0. 10.
5
6 Seed 64
```

Figure 48: An example of event file for the P-wave plot in Fig.??

Changed the second number column in line 3, 6.

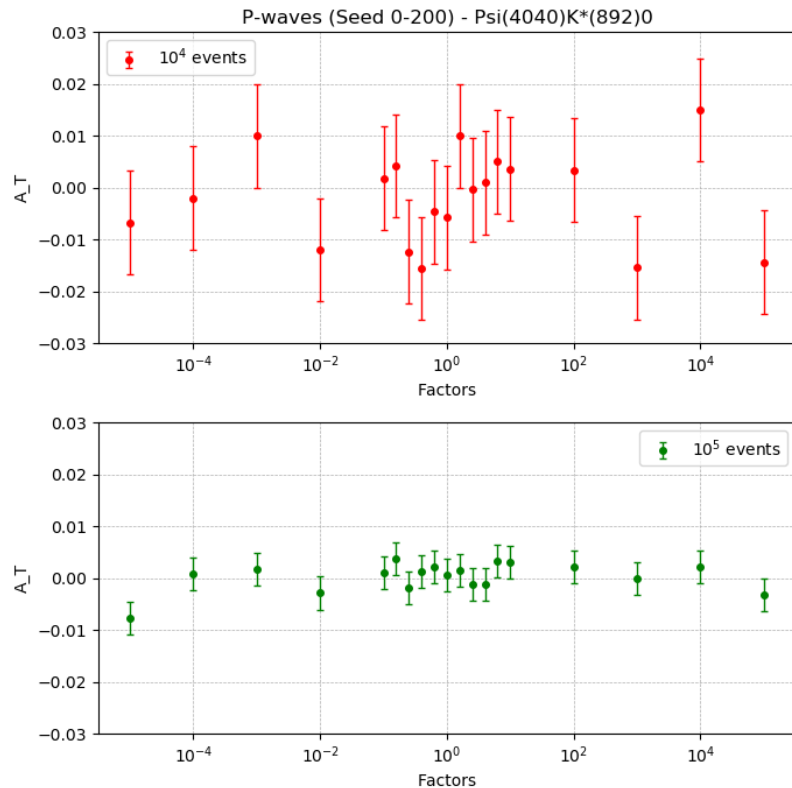


Figure 49: The change of A_T by multiplying the P wave amplitudes with the factors in x-axis using 10^4 and 10^5 events.

Put the results for $\psi(4040)\text{K}^*(892)0$ together with more events for the **E** and **F(1)** methods, this gives

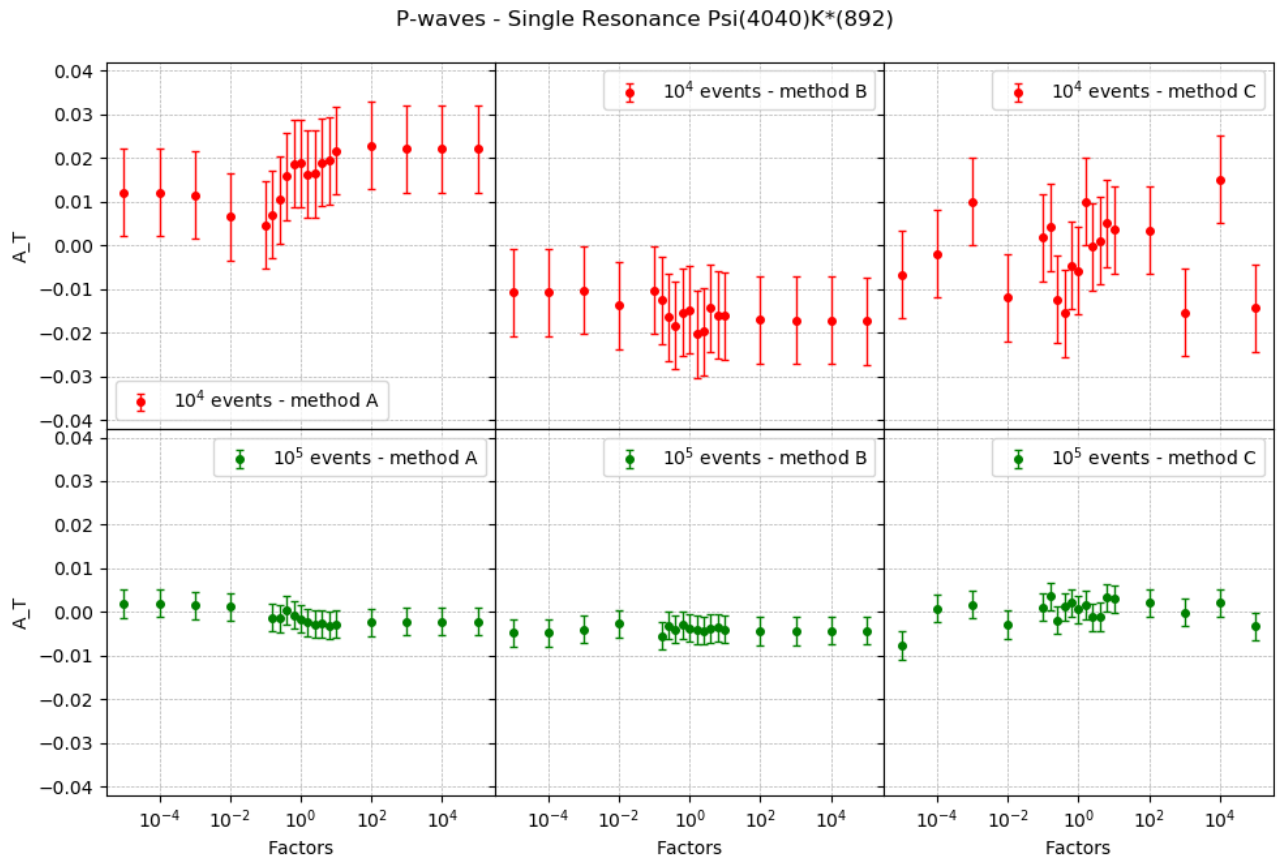


Figure 50: The change of A_T by multiplying the P wave amplitudes with the factors in x-axis using 10^4 and 10^5 events by generating events using three different methods.

More investigation on single resonance $\psi(3770)K^*(892)0$ using the methods stated in **E**, **F(1)** and **F(2)**.

Input files: AmpGen/build/bin/B0_event_spd_sr3_3770

Output files: Simulations/B02DDbarKPi/spd_waves_sr_3770

event file (.opt) Example:

(It was found we didn't specify the coordinate system in the event files. However, this doesn't effect the previous results since all the results were generated from real numbers - no phases)
We should also tell the units for the phase - I use radian.

```
~/AmpGen/build/bin/B0_event_spd_sr3_3770/B0toDbar0K+pi-.sr1.p.10000.opt
1 EventType B0 D0 Dbar0 K+ pi-
2
3 CouplingConstant::Coordinates polar
4
5 CouplingConstant::AngularUnits rad
6
7 B0[P]{psi(3770)0{D0,Dbar0},K*(892)0{K+,pi-}} 2 209300.000000000000000 0.0500000000000000 2 0.000000000000000 10.0000000000000000000
8 B0[S]{psi(3770)0{D0,Dbar0},K*(892)0{K+,pi-}} 2 2.093000000000000 0.050000000000000 2 0.000000000000000 10.0000000000000000000
```

Figure 51: An example of event file for the P-wave plot in Fig.52

Changed the second number column in line 7.

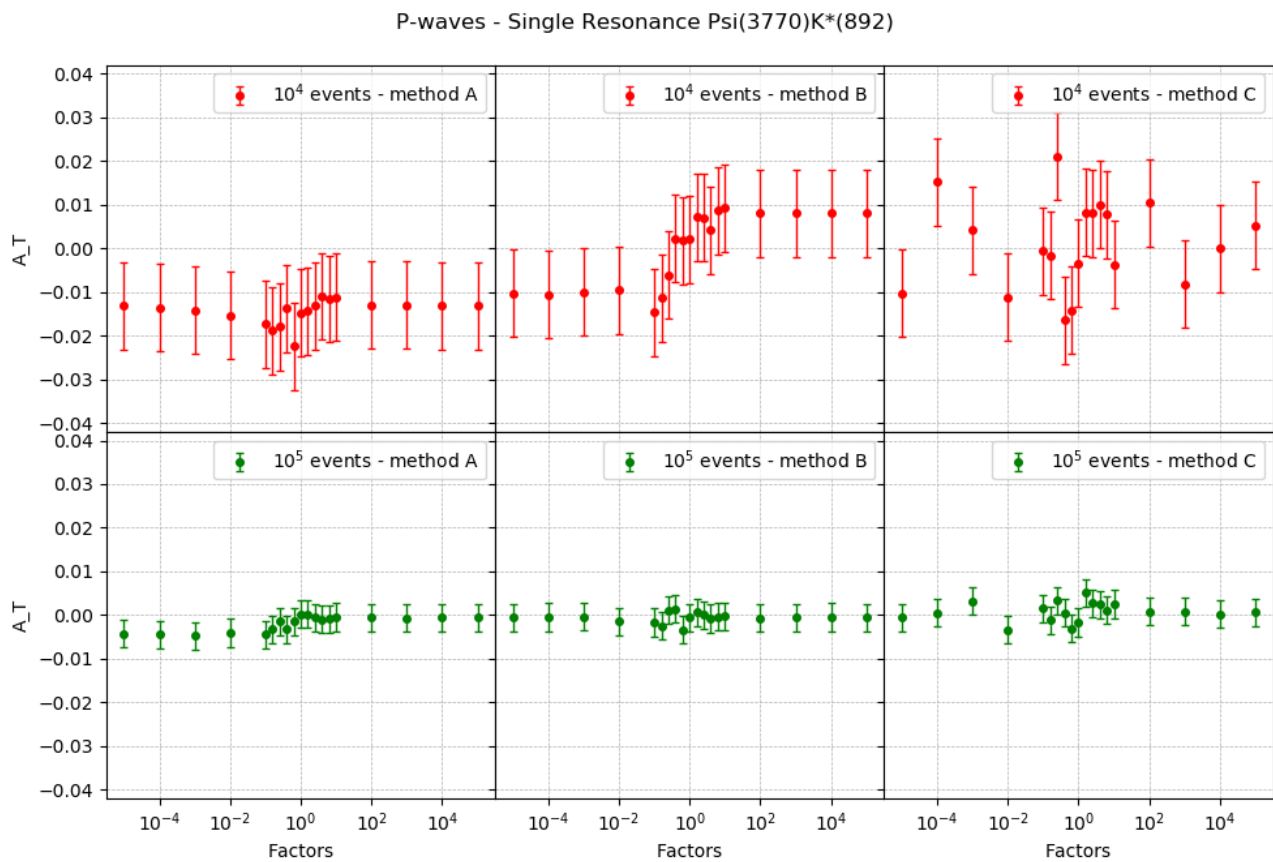


Figure 52: The change of A_T by multiplying the P wave amplitudes with the factors in x-axis using 10^4 and 10^5 events by generating events using three different methods.

Method A = **E**

Method B = **F(1)**

Method C = **F(2)**

More investigation on all resonance using the methods stated in F(2).

Input files: AmpGen/build/bin/B0_event_spd_nophase

Output files: Simulations/B02DDbarKPi/spd_waves_combine3_1E4 + spd_waves_combine3_1E5 + spd_waves_combine3_1E6

event file (.opt) Example:

```

~/AmpGen/build/bin/B0_event_spd_nophase/B0toDbar0K+pi-.p.opt
1 EventType B0 D0 Dbar0 K+ pi-
2
3 CouplingConstant::Coordinates polar
4
5 CouplingConstant::AngularUnits rad
6
7 B0[P]{psi(3770){D0,Dbar0},K*(892){K+,pi-}} 2 13.205937219970446 0.0500000000000000 2.00000000000000 0.00000000000000 10.00000000000000
8 B0[P]{psi(4040){D0,Dbar0},K*(892){K+,pi-}} 0 5.211707665406396 0.0500000000000000 0.00000000000000 0.00000000000000 10.00000000000000
9 B0[P]{psi(4160){D0,Dbar0},K*(892){K+,pi-}} 0 8.265541212690533 0.0500000000000000 0.00000000000000 0.00000000000000 10.00000000000000
10 B0[P]{psi(4415){D0,Dbar0},K*(892){K+,pi-}} 0 3.217882456848986 0.0500000000000000 0.00000000000000 0.00000000000000 10.00000000000000
11
12 B0[S]{psi(3770){D0,Dbar0},K*(892){K+,pi-}} 2 2.093000000000000 0.0500000000000000 2.00000000000000 0.00000000000000 10.00000000000000
13 B0[D]{psi(3770){D0,Dbar0},K*(892){K+,pi-}} 2 2.093000000000000 0.0500000000000000 2.00000000000000 0.00000000000000 10.00000000000000
14 B0[S]{psi(4040){D0,Dbar0},K*(892){K+,pi-}} 0 0.826000000000000 0.0500000000000000 0.00000000000000 0.00000000000000 10.00000000000000
15 B0[D]{psi(4040){D0,Dbar0},K*(892){K+,pi-}} 0 0.826000000000000 0.0500000000000000 0.00000000000000 0.00000000000000 10.00000000000000
16 B0[S]{psi(4160){D0,Dbar0},K*(892){K+,pi-}} 0 1.310000000000000 0.0500000000000000 0.00000000000000 0.00000000000000 10.00000000000000
17 B0[D]{psi(4160){D0,Dbar0},K*(892){K+,pi-}} 0 1.310000000000000 0.0500000000000000 0.00000000000000 0.00000000000000 10.00000000000000
18 B0[S]{psi(4415){D0,Dbar0},K*(892){K+,pi-}} 0 0.510000000000000 0.0500000000000000 0.00000000000000 0.00000000000000 10.00000000000000
19 B0[D]{psi(4415){D0,Dbar0},K*(892){K+,pi-}} 0 0.510000000000000 0.0500000000000000 0.00000000000000 0.00000000000000 10.00000000000000
20
21 B0{NonResS0{D0,Dbar0},K*(892){K+,pi-}} 0 2.090000000000000 1.000000000000000 0.00000000000000 0.00000000000000 10.00000000000000
22 B0{NonResS0{D0,Dbar0},K(0)*(1430){K+,pi-}} 0 0.660000000000000 1.000000000000000 0.00000000000000 0.00000000000000 10.00000000000000
23 B0{K(0)*(800){K+,pi-},NonResS0{D0,Dbar0}} 0 0.660000000000000 1.000000000000000 0.00000000000000 0.00000000000000 10.00000000000000
24 B0{D(s2)(2573)+D0,K},Dbar0,pi- 0 0.100000000000000 0.050000000000000 0.00000000000000 0.00000000000000 10.00000000000000
25
26 B0{psi(3770){D0,Dbar0},K(0)*(800){K+,pi-}} 0 1.990000000000000 0.0500000000000000 0.00000000000000 0.00000000000000 10.00000000000000
27 B0{psi(4040){D0,Dbar0},K(0)*(800){K+,pi-}} 0 0.780000000000000 0.0500000000000000 0.00000000000000 0.00000000000000 10.00000000000000
28 B0{psi(4160){D0,Dbar0},K(0)*(800){K+,pi-}} 0 1.240000000000000 0.0500000000000000 0.00000000000000 0.00000000000000 10.00000000000000
29 B0{psi(4415){D0,Dbar0},K(0)*(800){K+,pi-}} 0 0.480000000000000 0.0500000000000000 0.00000000000000 0.00000000000000 10.00000000000000
30
31 B0{psi(3770){D0,Dbar0},K(0)*(1430){K+,pi-}} 0 1.990000000000000 0.0500000000000000 0.00000000000000 0.00000000000000 10.00000000000000
32 B0{psi(4040){D0,Dbar0},K(0)*(1430){K+,pi-}} 0 0.780000000000000 0.0500000000000000 0.00000000000000 0.00000000000000 10.00000000000000
33 B0{psi(4160){D0,Dbar0},K(0)*(1430){K+,pi-}} 0 1.240000000000000 0.0500000000000000 0.00000000000000 0.00000000000000 10.00000000000000
34 B0{psi(4415){D0,Dbar0},K(0)*(1430){K+,pi-}} 0 0.480000000000000 0.0500000000000000 0.00000000000000 0.00000000000000 10.00000000000000
35
36 #B0/Z(c)(3900)+D*(2010)+{D0,pi+},Dbar0,K- 2 1.000000000000000 0.000000000000000 2.000000000000000 0.000000000000000 0.000000000000000

```

Figure 53: An example of event file for the P-wave plot in Fig.54

Changed the second number column in line 7, 8, 9, 10.

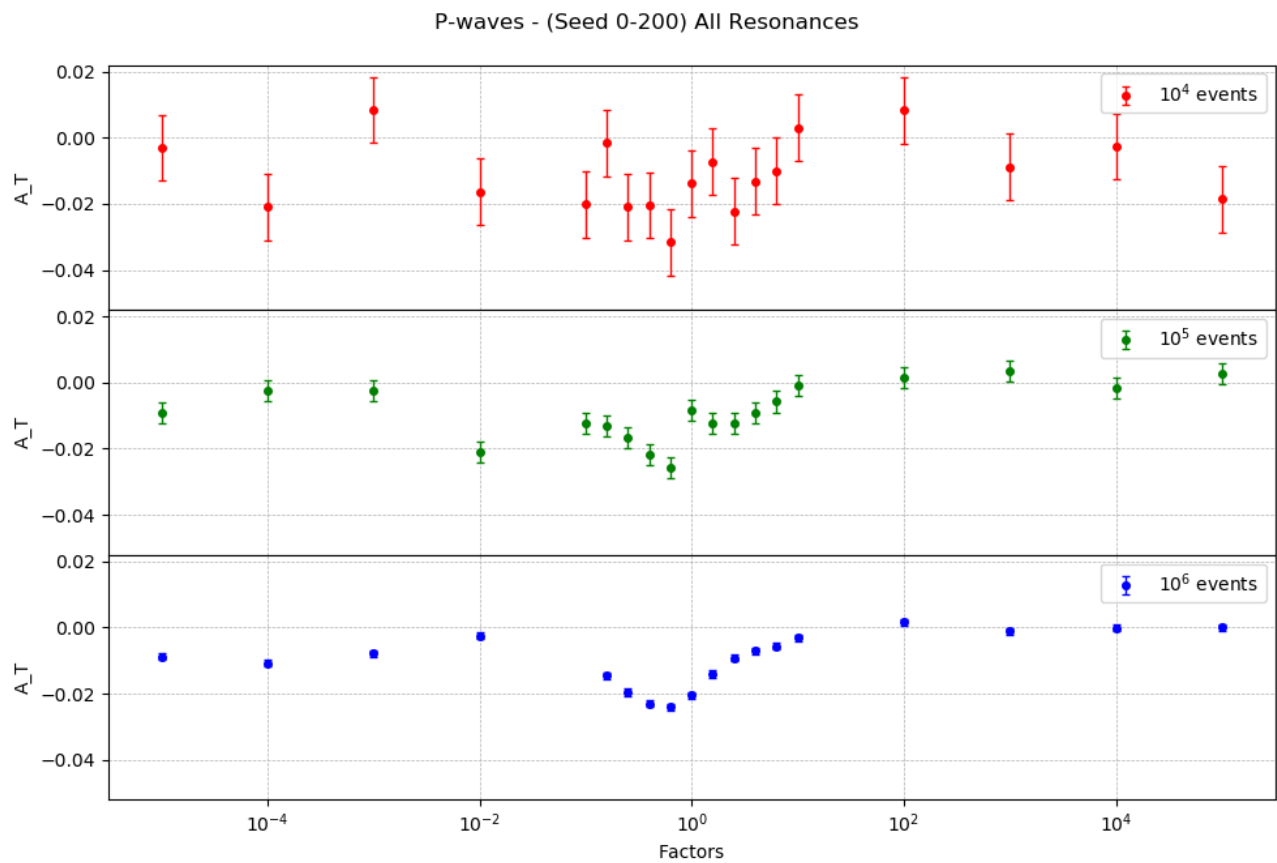


Figure 54: The change of A_T by multiplying the P wave amplitudes with the factors in x-axis using 10^4 , 10^5 and 10^6 events.

Start varying the phase of the resonance. The phase are chosen to be from -1.5π to 1.75π with intervals of 0.25π

For the single resonance - $\psi(3770)K^*(892)0$,

Input files: AmpGen/build/bin/B0_event_sr1_p_phase_1E5

Output files: Simulations/B02DDbarKPi/spd_waves_combine_phase_1E5

event file (.opt) Example:

```
~/AmpGen/build/bin/B0_event_sr1_p_phase_1E5/B0toDDbar0K+pi-_p.opt
1 |Event Type B0 D0 Dbar0 K+ pi-
2
3 CouplingConstant::Coordinates polar
4
5 CouplingConstant::AngularUnits rad
6
7 B0[P]{psi(3770)0{D0,Dbar0},K*(892)0{K+,pi-}} 2 209300.0000000000000000 0.0500000000000000 2 5.497787143782139 10.00000000000000
8 B0[S]{psi(3770)0{D0,Dbar0},K*(892)0{K+,pi-}} 2 2.093000000000000 0.0500000000000000 2 0.00000000000000 10.00000000000000
```

Figure 55: An example of event file for the P-wave plot in Fig.56

Changed the second and the fifth number column in line 7.

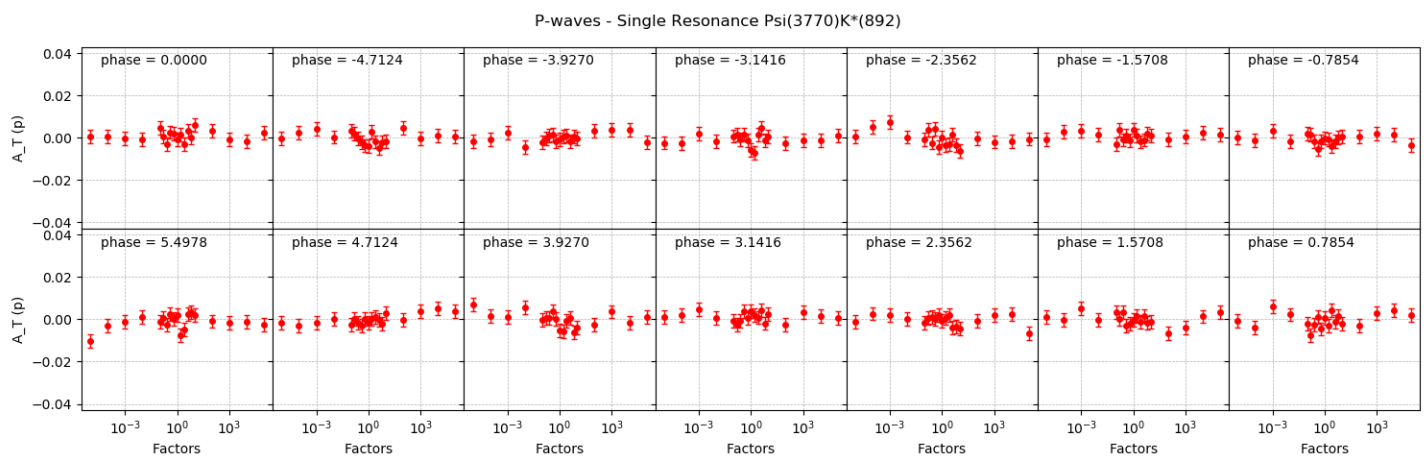


Figure 56: The change of A_T by multiplying the P wave amplitudes with the factors in x-axis using and changing the phase with 10^5 events.

- No obvious parity violation in this single resonance?

The whole process takes 22+7 hours. Would need some optimization in the codes for calculating A_T .

Have looked at the fitter in AmpGen by first generate 1000 events using AmpGen and fit the results with SignalOnlyFitter:

SignalOnlyFitter

An example fitter is provided in `examples/SignalOnlyFitter.cpp`, which as the name suggests only has a single signal component in the fit. The free parameters of the fit are specified in the same way as the Generator, with the additional relevant slots being `DataSample` which specifies the signal sample to fit, which is presumed to already have the selection applied, and `Branches` which takes a list of branch names, and defaults to the format used by the Generator etc. More details can be found with

```
SignalOnlyFitter --help
```

For example, the fitter can be used to fit a toy MC sample generated by the generator by running:

```
Generator MyOpts.opt --nEvents 100000
SignalOnlyFitter MyOpts.opt --DataSample Generate_Output.root
```

Figure 57: Instruction of using SignalOnlyFitter

The was done by unfixing (`fix=0`) the amplitudes and phases of the resonance in the `spd` event file and leaving only one resonance fixed. Here fixing $\psi(3770)K^*(892)0[S]$ (set to be `fix=2`) for both amplitude and phase.

The fitting returns back the real and imaginary part of the amplitude in the resonances of the decay and percentage/probability for the each resonance to occur, based on the four momentum data. This also generates a `plot.root` file containing the phase space plots. It takes about 5 minutes to finish the fitting for 10000 events.

A comparison was made between the generated MC data and the results from the amplitude fitting, as shown below:

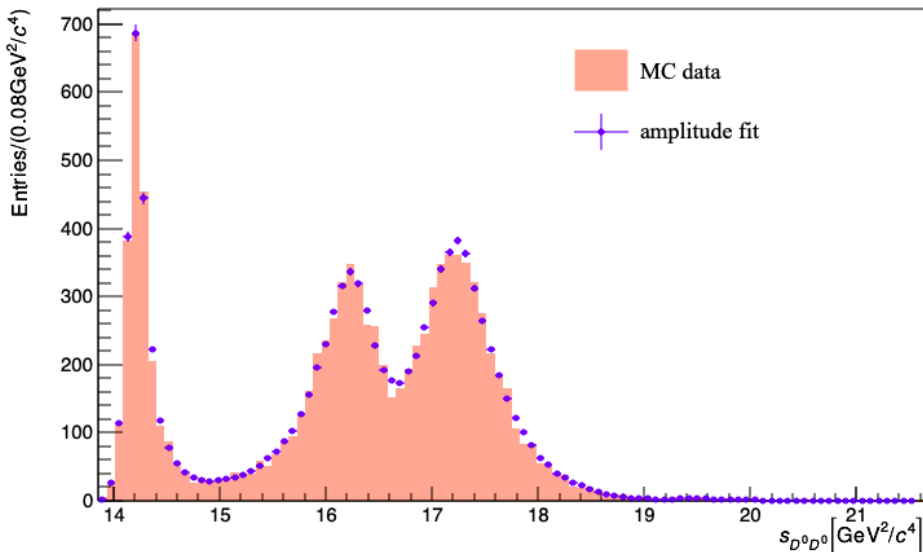


Figure 58: The verification of the fitter with the generated B^0 decays with 10000 events.

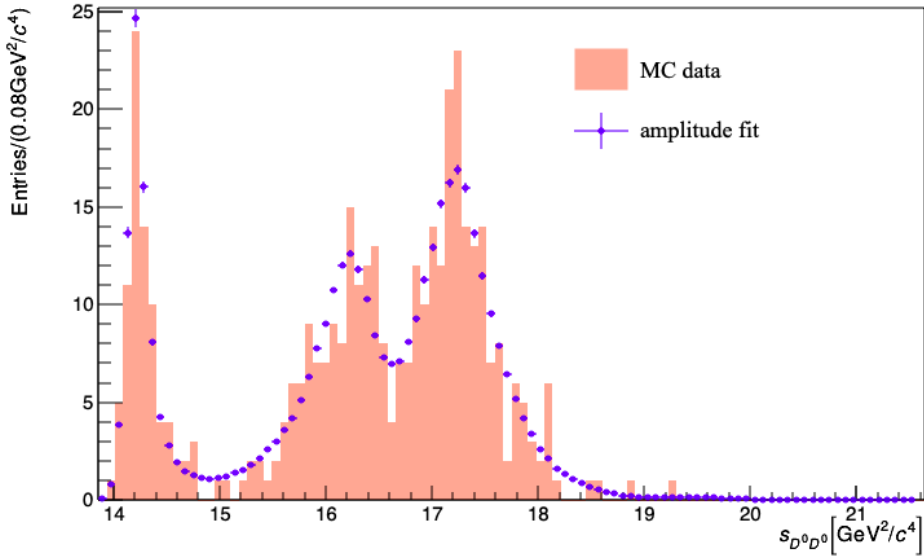


Figure 59: The verification of the fitter with the generated B^0 decays with 400 events (much fewer events).

The comparison of the ratio of the resonances contributed obtained from the fittings were made for different number of events using the Random Seed 7.

	400 events	1000 events	4000 events	10000 events	40000 events
$B0[P]\{\psi(4160)\{D0,Dbar0\},K*(892)\{K+,pi-\}\}$	$= 42.5 \pm 5.22 \%$	$42.02 \pm 3.5 \%$	$37.6 \pm 1.68 \%$	$36.62 \pm 1.05 \%$	$34.67 \pm 0.51 \%$
$B0[P]\{\psi(3770)\{D0,Dbar0\},K*(892)\{K+,pi-\}\}$	$= 19.46 \pm 2.98 \%$	$19.68 \pm 1.6 \%$	$21.77 \pm 0.82 \%$	$22.19 \pm 0.53 \%$	$21.59 \pm 0.26 \%$
$B0[P]\{\psi(4040)\{D0,Dbar0\},K*(892)\{K+,pi-\}\}$	$= 15.1 \pm 3.49 \%$	$15.69 \pm 2.2 \%$	$15.63 \pm 1.11 \%$	$16.74 \pm 0.71 \%$	$16.96 \pm 0.35 \%$
$B0[D]\{\psi(3770)\{D0,Dbar0\},K*(892)\{K+,pi-\}\}$	$= 3.33 \pm 1.3 \%$	$4.26 \pm 0.89 \%$	$5.44 \pm 0.49 \%$	$5.42 \pm 0.31 \%$	$5.27 \pm 0.15 \%$
$B0[S]\{\psi(4160)\{D0,Dbar0\},K*(892)\{K+,pi-\}\}$	$= 3.1 \pm 1.58 \%$	$3.73 \pm 0.88 \%$	$3.16 \pm 0.5 \%$	$2.93 \pm 0.24 \%$	$2.84 \pm 0.11 \%$
$B0[D]\{\psi(4160)\{D0,Dbar0\},K*(892)\{K+,pi-\}\}$	$= 2.51 \pm 1.46 \%$	$2.51 \pm 0.95 \%$	$3.06 \pm 0.38 \%$	$2.92 \pm 0.3 \%$	$2.79 \pm 0.14 \%$
$B0\{\psi(4160)\{D0,Dbar0\},K(0)*\{800\}\{K+,pi-\}\}$	$= 1.89 \pm 1.18 \%$	$2.25 \pm 0.86 \%$	$1.68 \pm 0.38 \%$	$1.46 \pm 0.14 \%$	$1.5 \pm 0.09 \%$
$B0\{\text{NonRes}S0\{D0,Dbar0\},K*(892)\{K+,pi-\}\}$	$= 1.3 \pm 0.85 \%$	$1.55 \pm 0.61 \%$	$1.61 \pm 0.3 \%$	$1.46 \pm 0.18 \%$	$1.48 \pm 0.07 \%$
$B0[S]\{\psi(4040)\{D0,Dbar0\},K*(892)\{K+,pi-\}\}$	$= 1.25 \pm 0.89 \%$	$1.49 \pm 0.62 \%$	$1.33 \pm 0.32 \%$	$1.24 \pm 0.16 \%$	$1.37 \pm 0.1 \%$
$B0[P]\{\psi(4415)\{D0,Dbar0\},K*(892)\{K+,pi-\}\}$	$= 0.82 \pm 0.85 \%$	$1.33 \pm 0.45 \%$	$1.33 \pm 0.29 \%$	$1.24 \pm 0.2 \%$	$1.19 \pm 0.08 \%$
$B0\{\psi(3770)\{D0,Dbar0\},K(0)*\{1430\}\{K+,pi-\}\}$	$= 0.76 \pm 0.56 \%$	$1.14 \pm 0.64 \%$	$1.19 \pm 0.21 \%$	$1.14 \pm 0.17 \%$	$1.16 \pm 0.08 \%$
$B0\{\psi(4160)\{D0,Dbar0\},K(0)*\{1430\}\{K+,pi-\}\}$	$= 0.71 \pm 0.78 \%$	$1.02 \pm 0.53 \%$	$1.13 \pm 0.25 \%$	$1 \pm 0.17 \%$	$0.99 \pm 0.08 \%$
$B0[K(0)*\{800\}\{K+,pi-\},\text{NonRes}S0\{D0,Dbar0\}\{K(0)*\{1430\}\{K+,pi-\}\}]$	$= 0.63 \pm 0.93 \%$	$0.89 \pm 0.49 \%$	$1.11 \pm 0.35 \%$	$0.95 \pm 0.16 \%$	$0.96 \pm 0.08 \%$
$B0[S]\{\psi(3770)\{D0,Dbar0\},K*(892)\{K+,pi-\}\}$	$= 0.54 \pm 0.71 \%$	$0.87 \pm 0.53 \%$	$0.79 \pm 0.24 \%$	$0.84 \pm 0.18 \%$	$0.67 \pm 0.07 \%$
$B0[D]\{\psi(4040)\{D0,Dbar0\},K*(892)\{K+,pi-\}\}$	$= 0.49 \pm 0.77 \%$	$0.83 \pm 0.64 \%$	$0.77 \pm 0.23 \%$	$0.8 \pm 0.16 \%$	$0.65 \pm 0.05 \%$
$B0\{\psi(3770)\{D0,Dbar0\},K(0)*\{800\}\{K+,pi-\}\}$	$= 0.49 \pm 0.63 \%$	$0.6 \pm 0.47 \%$	$0.73 \pm 0.25 \%$	$0.71 \pm 0.12 \%$	$0.64 \pm 0.08 \%$
$B0\{\text{NonRes}S0\{D0,Dbar0\},K(0)*\{1430\}\{K+,pi-\}\}$	$= 0.43 \pm 0.61 \%$	$0.55 \pm 0.41 \%$	$0.68 \pm 0.18 \%$	$0.7 \pm 0.14 \%$	$0.57 \pm 0.07 \%$
$B0\{\psi(4040)\{D0,Dbar0\},K(0)*\{800\}\{K+,pi-\}\}$	$= 0.37 \pm 0.62 \%$	$0.53 \pm 0.38 \%$	$0.66 \pm 0.26 \%$	$0.63 \pm 0.16 \%$	$0.47 \pm 0.06 \%$
$B0[D]\{\psi(4415)\{D0,Dbar0\},K*(892)\{K+,pi-\}\}$	$= 0.31 \pm 0.52 \%$	$0.41 \pm 0.38 \%$	$0.4 \pm 0.17 \%$	$0.44 \pm 0.11 \%$	$0.44 \pm 0.05 \%$
$B0\{\psi(4415)\{D0,Dbar0\},K(0)*\{1430\}\{K+,pi-\}\}$	$= 0.24 \pm 0.42 \%$	$0.28 \pm 0.34 \%$	$0.21 \pm 0.12 \%$	$0.11 \pm 0.05 \%$	$0.06 \pm 0.01 \%$
$B0\{\psi(4040)\{D0,Dbar0\},K(0)*\{1430\}\{K+,pi-\}\}$	$= 0.19 \pm 0.39 \%$	$0.16 \pm 0.27 \%$	$0.16 \pm 0.09 \%$	$0.08 \pm 0.04 \%$	$0.06 \pm 0.02 \%$
$B0[D(s2)(2573)+\{D0,K+\},Dbar0,pi-]$	$= 0.12 \pm 0.26 \%$	$0.13 \pm 0.2 \%$	$0.02 \pm 0.03 \%$	$0.03 \pm 0.03 \%$	$0.05 \pm 0.01 \%$
$B0[S]\{\psi(4415)\{D0,Dbar0\},K*(892)\{K+,pi-\}\}$	$= 0.07 \pm 0.23 \%$	$0.13 \pm 0.16 \%$	$0.02 \pm 0.04 \%$	$0.03 \pm 0.02 \%$	$0.02 \pm 0.01 \%$
$B0\{\psi(4415)\{D0,Dbar0\},K(0)*\{800\}\{K+,pi-\}\}$	$= 0.01 \pm 0.07 \%$	$0.02 \pm 0.08 \%$	$0.01 \pm 0.02 \%$	$0 \pm 0.01 \%$	$0.02 \pm 0.01 \%$
Sum_B0	$= 96.74 \pm 8.35 \%$	$102.21 \pm 4.74 \%$	$100.57 \pm 2.29 \%$	$99.79 \pm 1.4 \%$	$96.52 \pm 0.66 \%$

Figure 60: The ratio of the contributed resonances for generated MC data with different number of events.

Next steps:

- induce CP violation by change the number of C_T by several percent
- binned analysis for the CM variables
- real data from LHCb

28 March 2020, Friday

Start doing binned analysis following the method in the $D \rightarrow KK\pi\pi$ decay paper (add reference).

This uses the five CM variables as the phase-space variables and divides the phase-space into 32 regions with each region containing similar number of events.

The method is to divide the list of the first CM variable into two bins with equal number of events in each bin and find the bin edges. The next step is to apply the bin edges to the next CM variable, make it two bins and divide events in each bin into equal quantity which makes 4 bins in total. Repeating this, results in 32 bins for the 5th CM variable.

The next step is to allocate the triple products C_T of the events into regions in terms of a combination of the CM variable ranges obtained from the bin edges.

And then, the triple product asymmetries and CP asymmetries can be obtained from the C_T in each phase-space region.

For 10^5 events with all the resonances included and S,P,D waves applied to the spin-1 resonances, using the `f or` loop arrangement to allocate C_T into the phase-space regions, this gives the total number of C_T in each region:

[1422, 897, 1402, 905, 1387, 911, 1400, 905, 1401, 902, 1372, 911, 1400, 907, 1415, 899, 1458, 884, 1429, 893, 1395, 906, 1421, 892, 1444, 883, 1355, 920, 1380, 916, 1407, 902, 1222, 1940, 1204, 1969, 1187, 1973, 1199, 1965, 1203, 1977, 1187, 1991, 1198, 1971, 1205, 1952, 1237, 1907, 1222, 1932, 1192, 1966, 1211, 1937, 1224, 1923, 1178, 2012, 1185, 2002, 1201, 1959].

This summed over to give 87552 events, which is less than the original number of events. The reason might be that some events do not satisfy any arrangements of the phase-space variables in the 32 regions, and hence were miscounted.

This gives The bin arrangement:

(0.00,1.58)	(3.73,4.05)	(0.63,0.90)	(-1.00,0.00)	(-1.00,0.01)
(1.58,3.14)	(4.05,4.62)	(0.90,1.51)	(0.00,1.00)	(0.01,1.00)
(0.00,1.58)	(3.73,4.05)	(0.63,0.90)	(-1.00,0.00)	(-1.00,0.00)
(1.58,3.14)	(4.05,4.63)	(0.90,1.50)	(0.00,1.00)	(0.00,1.00)
(0.00,1.58)	(3.73,4.05)	(0.63,0.90)	(-1.00,-0.01)	(-1.00,0.02)
(1.58,3.14)	(4.05,4.62)	(0.90,1.50)	(-0.01,1.00)	(0.02,1.00)
(0.00,1.58)	(3.73,4.05)	(0.63,0.90)	(-1.00,-0.01)	(-1.00,-0.00)
(1.58,3.14)	(4.05,4.63)	(0.90,1.50)	(-0.01,1.00)	(-0.00,1.00)
(0.00,1.58)	(3.73,4.05)	(0.63,0.90)	(-1.00,0.00)	(-1.00,0.00)
(1.58,3.14)	(4.05,4.62)	(0.90,1.51)	(0.00,1.00)	(0.00,1.00)
(0.00,1.58)	(3.73,4.05)	(0.63,0.90)	(-1.00,-0.01)	(-1.00,0.01)
(1.58,3.14)	(4.05,4.63)	(0.90,1.50)	(-0.01,1.00)	(0.01,1.00)
(0.00,1.58)	(3.73,4.05)	(0.63,0.90)	(-1.00,0.00)	(-1.00,0.01)
(1.58,3.14)	(4.05,4.62)	(0.90,1.50)	(0.00,1.00)	(0.01,1.00)
(0.00,1.58)	(3.73,4.05)	(0.63,0.90)	(-1.00,-0.01)	(-1.00,0.00)
(1.58,3.14)	(4.05,4.63)	(0.90,1.50)	(-0.01,1.00)	(0.00,1.00)
(0.00,1.58)	(3.73,4.05)	(0.63,0.90)	(-1.00,0.00)	(-1.00,0.02)
(1.58,3.14)	(4.05,4.62)	(0.90,1.51)	(0.00,1.00)	(0.02,1.00)
(0.00,1.58)	(3.73,4.05)	(0.63,0.90)	(-1.00,0.00)	(-1.00,0.01)
(1.58,3.14)	(4.05,4.63)	(0.90,1.50)	(-0.01,1.00)	(0.01,1.00)
(0.00,1.58)	(3.73,4.05)	(0.63,0.90)	(-1.00,0.00)	(-1.00,0.02)
(1.58,3.14)	(4.05,4.62)	(0.90,1.50)	(0.00,1.00)	(0.01,1.00)
(0.00,1.58)	(3.73,4.05)	(0.63,0.90)	(-1.00,-0.01)	(-1.00,0.02)
(1.58,3.14)	(4.05,4.63)	(0.90,1.50)	(-0.01,1.00)	(0.02,1.00)
(0.00,1.58)	(3.73,4.05)	(0.63,0.90)	(-1.00,-0.01)	(-1.00,0.01)
(1.58,3.14)	(4.05,4.63)	(0.90,1.50)	(-0.01,1.00)	(0.01,1.00)
(0.00,1.58)	(3.73,4.05)	(0.63,0.90)	(-1.00,0.00)	(-1.00,0.02)
(1.58,3.14)	(4.05,4.62)	(0.90,1.51)	(0.00,1.00)	(0.02,1.00)
(0.00,1.58)	(3.73,4.05)	(0.63,0.90)	(-1.00,-0.01)	(-1.00,0.01)
(1.58,3.14)	(4.05,4.63)	(0.90,1.50)	(-0.01,1.00)	(0.01,1.00)
(0.00,1.58)	(3.73,4.05)	(0.63,0.90)	(-1.00,0.00)	(-1.00,0.02)
(1.58,3.14)	(4.05,4.62)	(0.90,1.51)	(0.00,1.00)	(0.02,1.00)
(0.00,1.58)	(3.73,4.05)	(0.63,0.90)	(-1.00,-0.01)	(-1.00,-0.00)
(1.58,3.14)	(4.05,4.63)	(0.90,1.50)	(-0.01,1.00)	(-0.00,1.00)
(0.00,1.58)	(3.73,4.05)	(0.63,0.90)	(-1.00,0.00)	(-1.00,0.00)
(1.58,3.14)	(4.05,4.62)	(0.90,1.50)	(-0.01,1.00)	(-0.00,1.00)

Figure 61: The 32 regions of the five-dimensional phase space of the four-body, as in the order of: ϕ , $m(D^0\bar{D}^0)$, $m(K\pi)$, $\cos(\theta_D)$, $\cos(\theta_K)$.

The asymmetry distributions are:

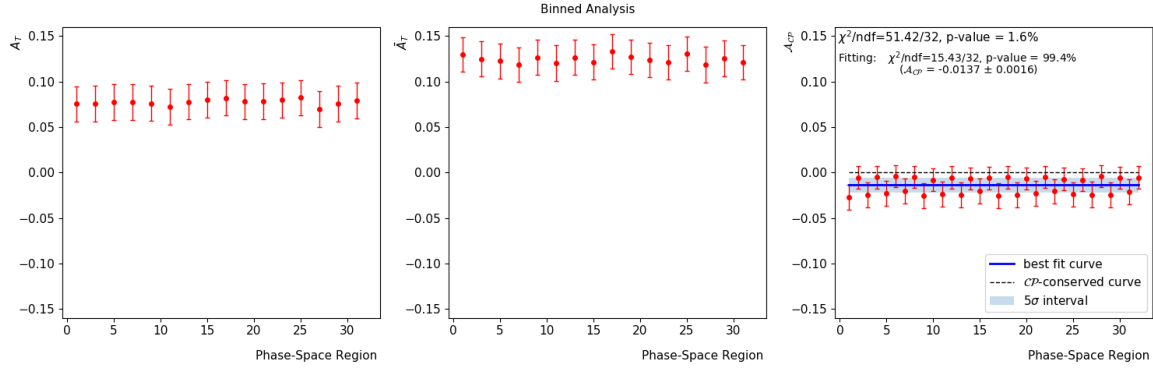


Figure 62: The distribution of the asymmetries using the binning scheme.

The events are generated using all resonances with the S,P,D waves included for the spin-1 resonances, and 10 random seeds. This changes the distributions of CM variables without S,P,D waves using one seed only:

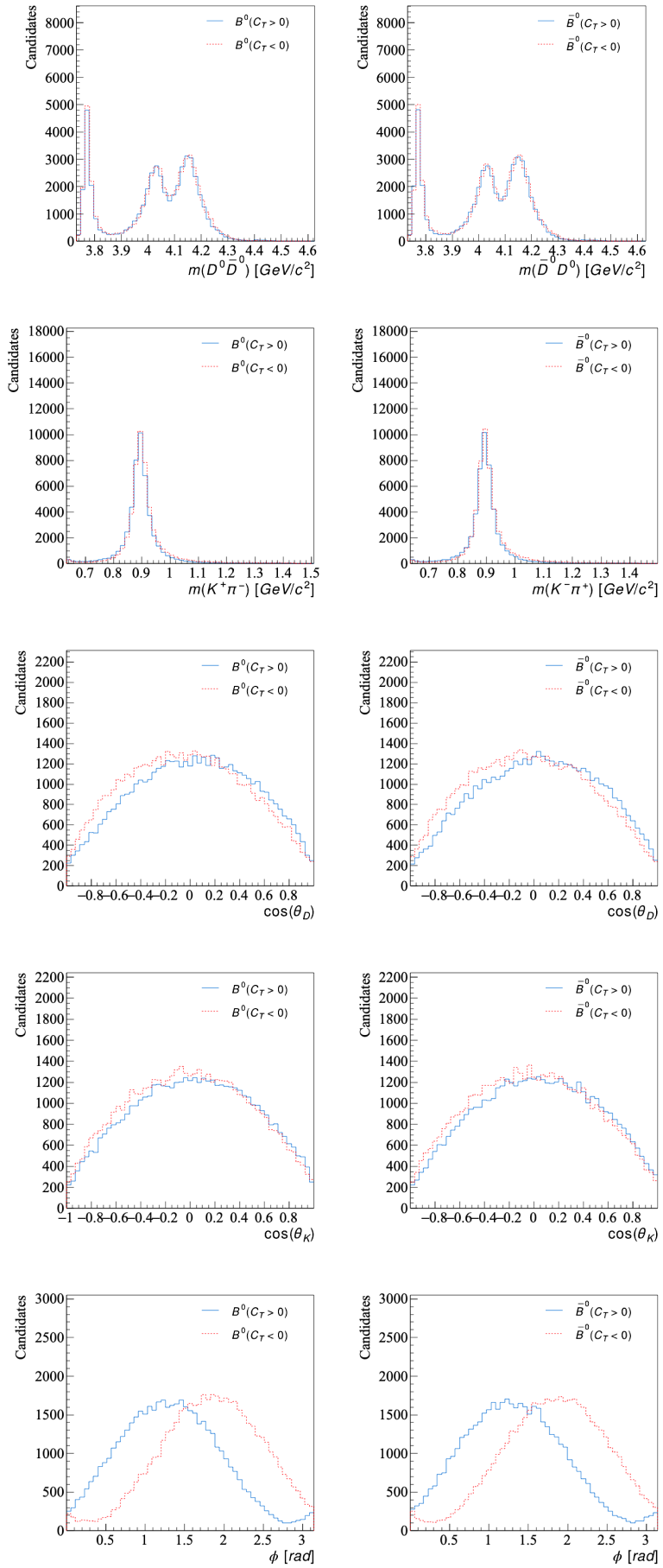


Figure 63: The CM variable distribution for the model with spd waves using 10 different random seeds.

The code is developed to allow different bin arrangements for the 32 phase space regions.

An alternative is:

(0.00,1.58)	(3.73,4.05)	(0.63,0.90)	(-1.00,0.00)	(-1.00,0.01)
(0.00,1.58)	(3.73,4.05)	(0.63,0.90)	(-1.00,0.00)	(0.01,1.00)
(0.00,1.58)	(3.73,4.05)	(0.63,0.90)	(0.00,1.00)	(-1.00,0.00)
(0.00,1.58)	(3.73,4.05)	(0.63,0.90)	(0.00,1.00)	(0.00,1.00)
(0.00,1.58)	(3.73,4.05)	(0.90,1.51)	(-1.00,0.00)	(-1.00,0.02)
(0.00,1.58)	(3.73,4.05)	(0.90,1.51)	(-1.00,0.00)	(0.02,1.00)
(0.00,1.58)	(3.73,4.05)	(0.90,1.51)	(0.00,1.00)	(-1.00,-0.00)
(0.00,1.58)	(3.73,4.05)	(0.90,1.51)	(0.00,1.00)	(-0.00,1.00)
(0.00,1.58)	(4.05,4.62)	(0.63,0.90)	(-1.00,-0.01)	(-1.00,0.00)
(0.00,1.58)	(4.05,4.62)	(0.63,0.90)	(-1.00,-0.01)	(0.00,1.00)
(0.00,1.58)	(4.05,4.62)	(0.63,0.90)	(-0.01,1.00)	(-1.00,0.01)
(0.00,1.58)	(4.05,4.62)	(0.63,0.90)	(-0.01,1.00)	(0.01,1.00)
(0.00,1.58)	(4.05,4.62)	(0.90,1.50)	(-1.00,-0.01)	(-1.00,0.01)
(0.00,1.58)	(4.05,4.62)	(0.90,1.50)	(-1.00,-0.01)	(0.01,1.00)
(0.00,1.58)	(4.05,4.62)	(0.90,1.50)	(-0.01,1.00)	(-1.00,0.00)
(0.00,1.58)	(4.05,4.62)	(0.90,1.50)	(-0.01,1.00)	(0.00,1.00)
(1.58,3.14)	(3.73,4.05)	(0.63,0.90)	(-1.00,0.00)	(-1.00,0.02)
(1.58,3.14)	(3.73,4.05)	(0.63,0.90)	(-1.00,0.00)	(0.02,1.00)
(1.58,3.14)	(3.73,4.05)	(0.63,0.90)	(0.00,1.00)	(-1.00,0.01)
(1.58,3.14)	(3.73,4.05)	(0.63,0.90)	(0.00,1.00)	(0.01,1.00)
(1.58,3.14)	(3.73,4.05)	(0.90,1.50)	(-1.00,-0.01)	(-1.00,0.02)
(1.58,3.14)	(3.73,4.05)	(0.90,1.50)	(-1.00,-0.01)	(0.02,1.00)
(1.58,3.14)	(3.73,4.05)	(0.90,1.50)	(-0.01,1.00)	(-1.00,0.01)
(1.58,3.14)	(3.73,4.05)	(0.90,1.50)	(-0.01,1.00)	(0.01,1.00)
(1.58,3.14)	(4.05,4.63)	(0.63,0.90)	(-1.00,0.00)	(-1.00,0.02)
(1.58,3.14)	(4.05,4.63)	(0.63,0.90)	(-1.00,0.00)	(0.02,1.00)
(1.58,3.14)	(4.05,4.63)	(0.63,0.90)	(0.00,1.00)	(-1.00,-0.00)
(1.58,3.14)	(4.05,4.63)	(0.63,0.90)	(0.00,1.00)	(-0.00,1.00)
(1.58,3.14)	(4.05,4.63)	(0.90,1.50)	(-1.00,-0.00)	(-1.00,0.00)
(1.58,3.14)	(4.05,4.63)	(0.90,1.50)	(-1.00,-0.00)	(0.00,1.00)
(1.58,3.14)	(4.05,4.63)	(0.90,1.50)	(-0.00,1.00)	(-1.00,-0.00)
(1.58,3.14)	(4.05,4.63)	(0.90,1.50)	(-0.00,1.00)	(-0.00,1.00)

Figure 64: The 32 regions of the five-dimensional phase space of the four-body, as in the order of: ϕ , $m(D^0\bar{D}^0)$, $m(K\pi)$, $\cos(\theta_D)$, $\cos(\theta_K)$.

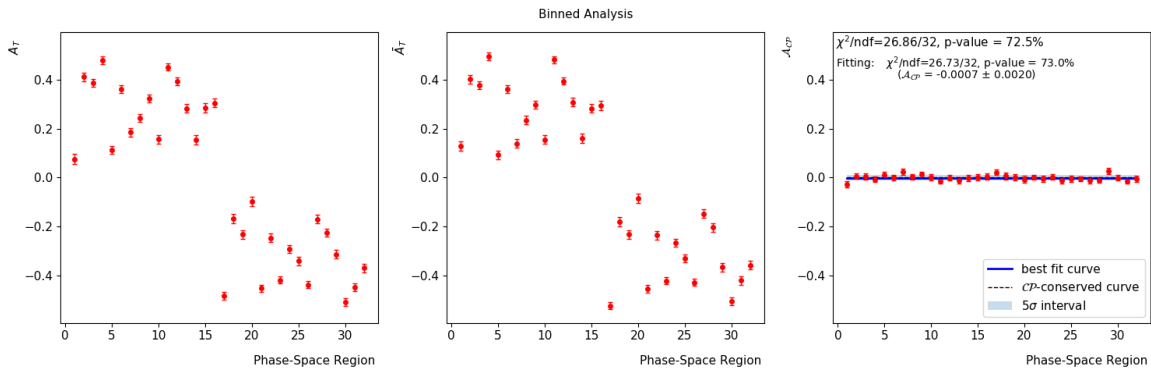


Figure 65: The distribution of the asymmetries using the binning scheme in Fig.64

And for the arrangements from the literature:

(0.00,1.58)	(3.73,4.05)	(0.63,0.90)	(-1.00,0.00)	(-1.00,0.01)
(0.00,1.58)	(3.73,4.05)	(0.90,1.51)	(-1.00,0.00)	(-1.00,0.00)
(0.00,1.58)	(4.05,4.62)	(0.63,0.90)	(-1.00,-0.01)	(-1.00,0.02)
(0.00,1.58)	(4.05,4.62)	(0.90,1.50)	(-1.00,-0.01)	(-1.00,-0.00)
(1.58,3.14)	(3.73,4.05)	(0.63,0.90)	(-1.00,0.00)	(-1.00,0.00)
(1.58,3.14)	(3.73,4.05)	(0.90,1.50)	(-1.00,-0.01)	(-1.00,0.01)
(1.58,3.14)	(4.05,4.63)	(0.63,0.90)	(-1.00,0.00)	(-1.00,0.01)
(1.58,3.14)	(4.05,4.63)	(0.90,1.50)	(-1.00,-0.00)	(-1.00,0.00)
(0.00,1.58)	(3.73,4.05)	(0.63,0.90)	(0.00,1.00)	(-1.00,0.02)
(0.00,1.58)	(3.73,4.05)	(0.90,1.51)	(0.00,1.00)	(-1.00,0.01)
(0.00,1.58)	(4.05,4.62)	(0.63,0.90)	(-0.01,1.00)	(-1.00,0.02)
(0.00,1.58)	(4.05,4.62)	(0.90,1.50)	(-0.01,1.00)	(-1.00,0.01)
(1.58,3.14)	(3.73,4.05)	(0.63,0.90)	(0.00,1.00)	(-1.00,0.02)
(1.58,3.14)	(3.73,4.05)	(0.90,1.50)	(-0.01,1.00)	(-1.00,-0.00)
(1.58,3.14)	(4.05,4.63)	(0.63,0.90)	(0.00,1.00)	(-1.00,0.00)
(1.58,3.14)	(4.05,4.63)	(0.90,1.50)	(-0.00,1.00)	(-1.00,-0.00)
(0.00,1.58)	(3.73,4.05)	(0.63,0.90)	(-1.00,0.00)	(0.01,1.00)
(0.00,1.58)	(3.73,4.05)	(0.90,1.51)	(-1.00,0.00)	(0.00,1.00)
(0.00,1.58)	(4.05,4.62)	(0.63,0.90)	(-1.00,-0.01)	(0.02,1.00)
(0.00,1.58)	(4.05,4.62)	(0.90,1.50)	(-1.00,-0.01)	(-0.00,1.00)
(1.58,3.14)	(3.73,4.05)	(0.63,0.90)	(-1.00,0.00)	(0.00,1.00)
(1.58,3.14)	(3.73,4.05)	(0.90,1.50)	(-1.00,-0.01)	(0.01,1.00)
(1.58,3.14)	(4.05,4.63)	(0.63,0.90)	(-1.00,0.00)	(0.01,1.00)
(1.58,3.14)	(4.05,4.63)	(0.90,1.50)	(-1.00,-0.00)	(0.00,1.00)
(0.00,1.58)	(3.73,4.05)	(0.63,0.90)	(0.00,1.00)	(-0.00,1.00)
(0.00,1.58)	(3.73,4.05)	(0.90,1.51)	(-0.00,1.00)	(-0.00,1.00)

Figure 66: The 32 regions of the five-dimensional phase space of the four-body, as in the order of: ϕ , $m(D^0\bar{D}^0)$, $m(K\pi)$, $\cos(\theta_D)$, $\cos(\theta_K)$.

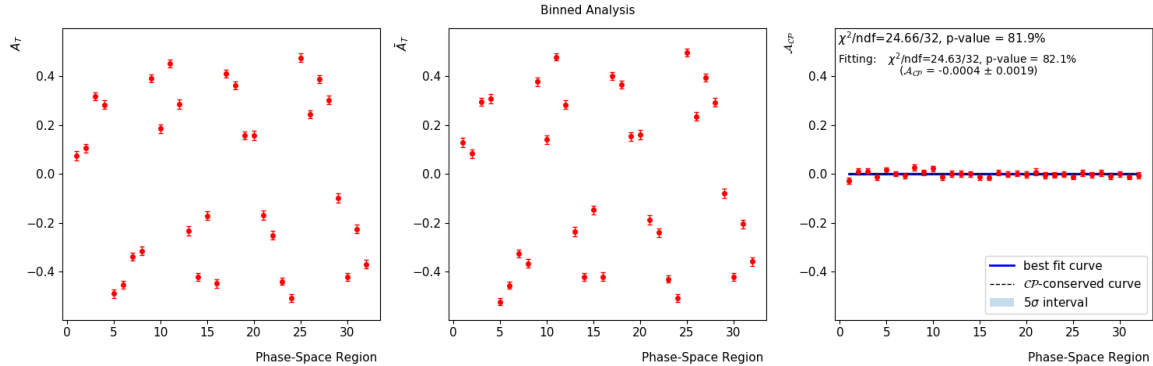


Figure 67: The distribution of the asymmetries using the binning scheme in Fig.66

First look of LHCb data (Run I):

The data contains the four momentum of the mother particle B^0 and the four daughter particles. The data for regular decay and charge-conjugate decay were split according to the value of `K_Kst0_ID`, in terms of 321 and -321, respectively. So, in the column of (e.g.) `D0_PX`, the value with ID=321 is the momentum of D^0 comes from the regular decay, while the value with ID=-321 is the momentum of D^0 comes from the conjugate decay. And similarly, in the column of `Dbar0_PX`, the value with ID=321 is the \bar{D}^0 comes from the regular decay and the value with ID=-321 is the \bar{D}^0 comes from the conjugate decay. The data were cut on for the classifier with `NN_weights > 0.9979`. The overall selection efficiency is 4.08×10^{-4} . The total number of data obtained is 2678 with 1405 being regular and 1273 being charge-conjugate process.

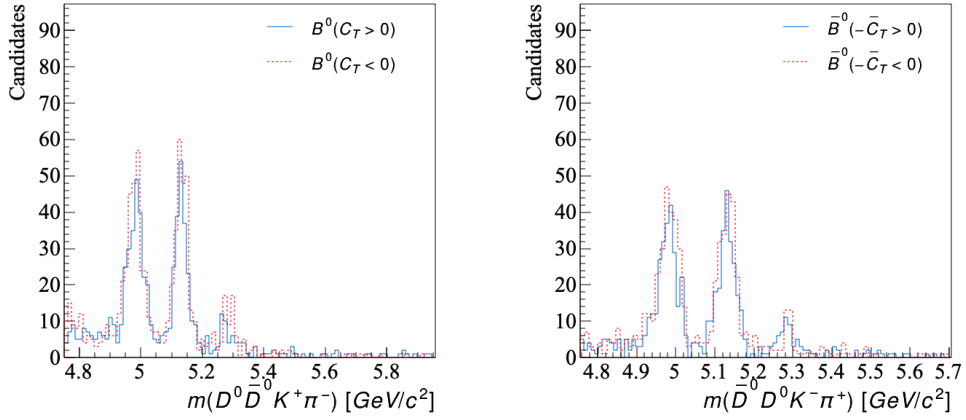


Figure 68: The invariant mass of $D^0\bar{D}^0K^+\pi^-$ and its conjugate decays with different values of the triple products C_T .

The resonance is expected to happen at around $5.28\text{GeV}/c^2$. It shows that there are some contributions from other sources: the background signal or the decays not coming from B^0 . The `sWeights = N_s / (N_s + N_b)` are required to add to the data, which accounts for the probability for a particular event signal comes from the B^0 decay. [It is not clear if the background was studied over the whole phase space or not either (if not, then the background subtraction is only an approximation and we'll have to make note of that)]. After applying the `sWeights` to the histogram, the background signal is removed, and shows the correct resonance distribution for B^0 with 115 events:

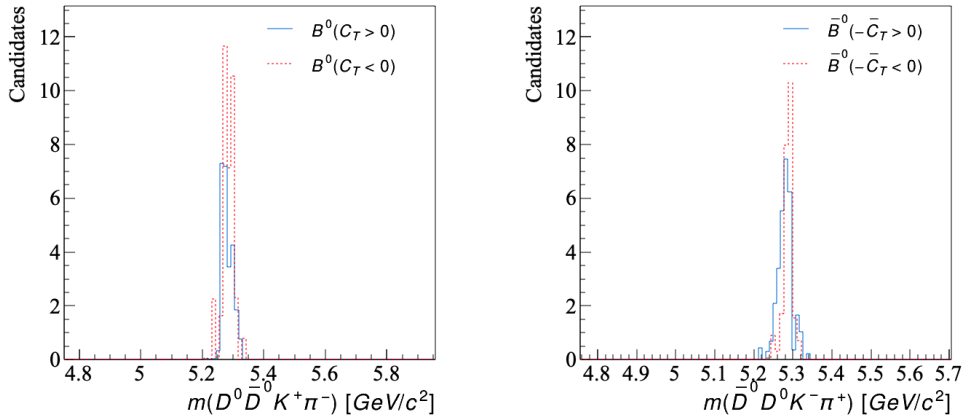


Figure 69: The invariant mass of $D^0\bar{D}^0K^+\pi^-$ and its conjugate decays with different values of the triple products C_T after applying the `sWeights`.

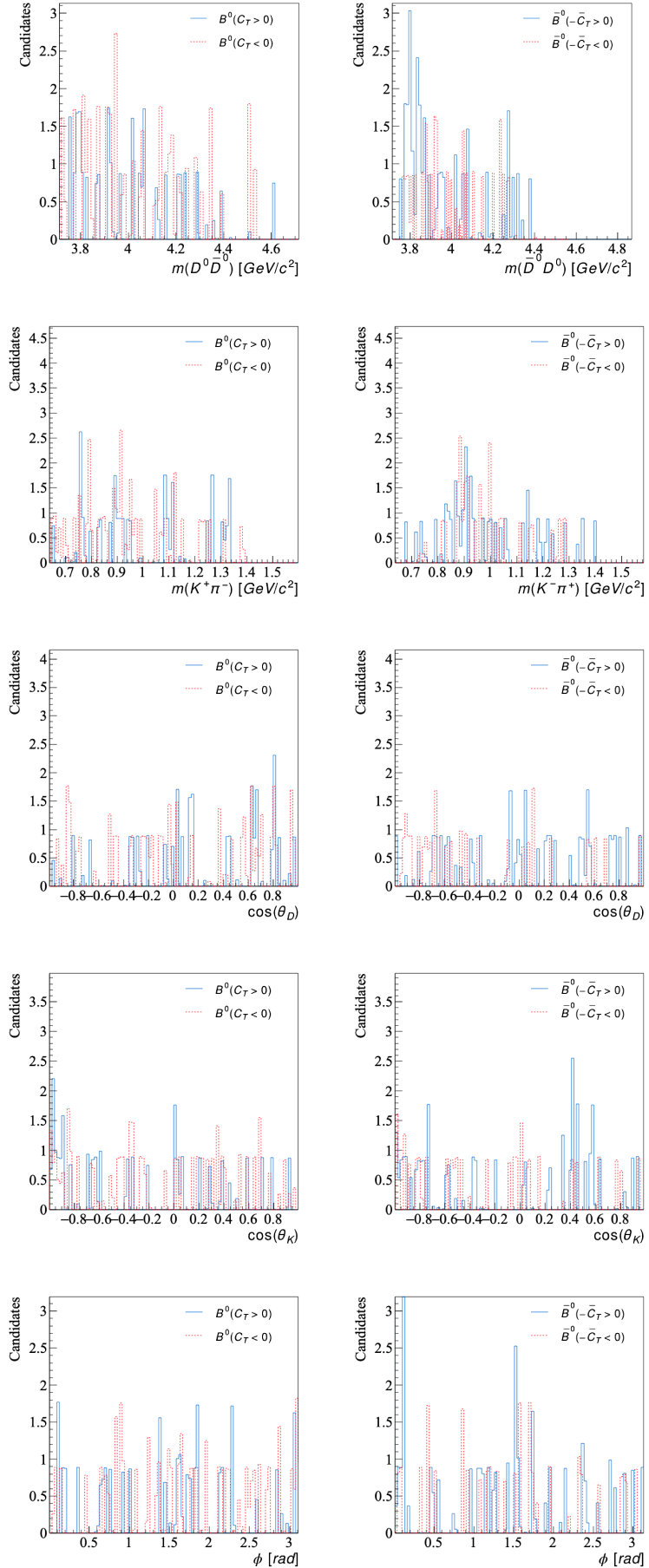


Figure 70: The distribution of the CM variable of the LHCb (Run I) data after adding the weights. This doesn't show an obvious correct distributions comparing to the previous simulated distribution in e.g. Fig.63. The reason might be the there are not enough number of events and the weights used in the B^0 decay doesn't apply to these variables.

This distribution of the weighted B^0 resonances are fitted using a Gaussian function:

$$f(x) = Ae^{-\frac{(x-x_0)^2}{2\sigma^2}}, \quad (6)$$

where A is the amplitude, x_0 is the mean and σ is the standard deviation of the distribution.

The fit gives

bin=100							
	A	err_A	mean	err_mean	sigma	err_sigma	type
B0	6.9500	0.3265	5.2761	0.0009	0.0171	0.0009	$B^0(C_T > 0)$
B0	10.6653	0.5292	5.2854	0.0009	0.0164	0.0009	$B^0(C_T < 0)$
B0	7.2257	0.2280	5.2806	0.0005	0.0141	0.0005	$\bar{B}^0(-C_T > 0)$
B0	10.7597	0.2029	5.2901	0.0002	0.0090	0.0002	$\bar{B}^0(-C_T < 0)$

Figure 71: The results of the parameters after fitting the B_0 resonance using the eq.6.

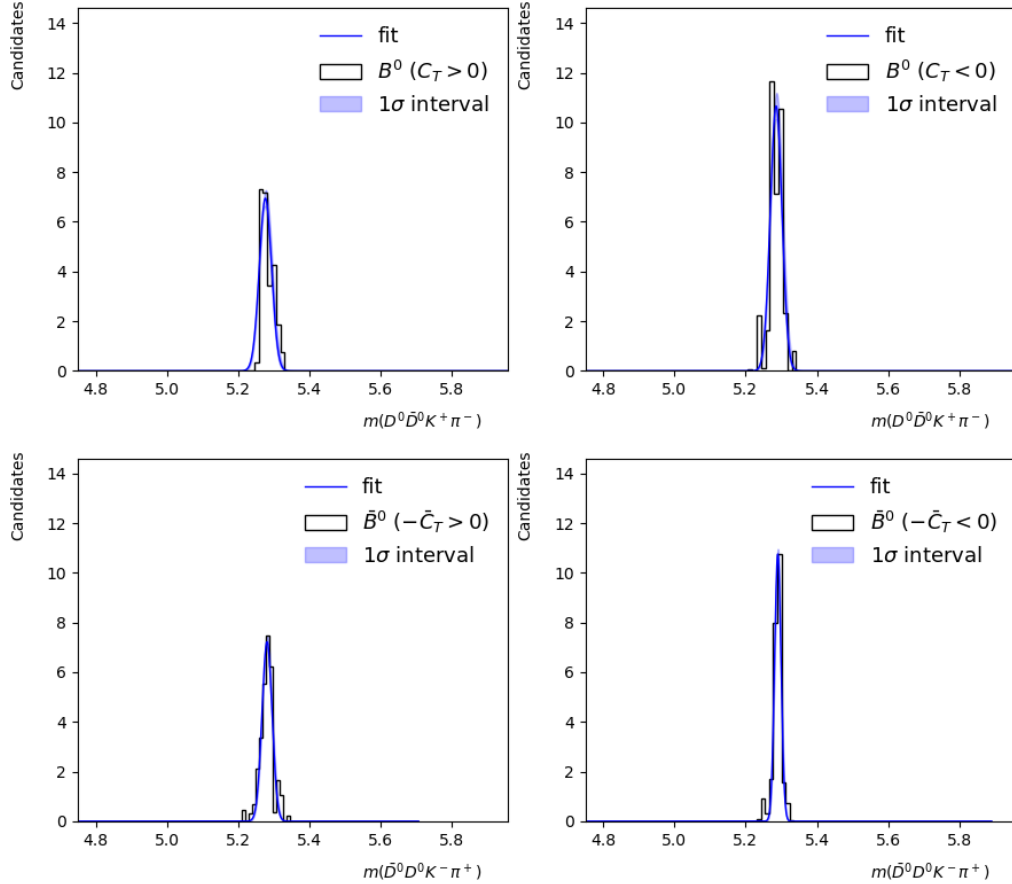


Figure 72: The fitted distribution of the B_0 resonance with showing the $1-\sigma$ tolerance.

To find the triple product and CP asymmetries for the LHCb data, the yields of the data for the four C_T cases were calculated. One way to calculate the yields is to find the integral of the Gaussian distribution (Eq.6) of the B^0 resonances in Fig.72 and divided by the bin width Δm . The calculation is given by:

$$\begin{aligned}
 \eta &= \frac{1}{\Delta m} \int_{-\infty}^{\infty} f(x) dx \\
 &= \frac{1}{\Delta m} \int_{-\infty}^{\infty} A e^{-\frac{(x-x_0)^2}{2\sigma^2}} dx \\
 &= \frac{A}{\Delta m} \int_{-\infty}^{\infty} e^{-ay^2} dy \quad y = x - x_0, a = \frac{1}{2\sigma^2} \\
 &= \frac{A}{\Delta m} \sqrt{\frac{\pi}{a}} = \frac{A\sigma}{\Delta m} \sqrt{2\pi}.
 \end{aligned} \tag{7}$$

The uncertainties for the yields are contributed from two sources: the uncertainty in the yields it self (which can be treated as a Poisson distribution) and the uncertainty from the fittings. The first uncertainty is then given by

$$\sigma_{\eta\text{-self}} = \sqrt{\eta}, \tag{8}$$

while the second uncertainty is found from partial derivatives:

$$\begin{aligned}
 \sigma_{\eta\text{-fit}} &= \sqrt{\left(\frac{\partial\eta}{\partial A}\Delta A\right)^2 + \left(\frac{\partial\eta}{\partial\sigma}\Delta\sigma\right)^2} \\
 &= \sqrt{\left(\eta \frac{\Delta A}{A}\right)^2 + \left(\eta \frac{\Delta\sigma}{\sigma}\right)^2} \\
 &= \eta \sqrt{\left(\frac{\Delta A}{A}\right)^2 + \left(\frac{\Delta\sigma}{\sigma}\right)^2}.
 \end{aligned} \tag{9}$$

Using the above equations to calculate η 's for the four Gaussian distribution gives the triple product and CP asymmetry for the regular and conjugate decay:

$$A_T = \frac{\eta(C_T > 0) - \eta(C_T < 0)}{\eta(C_T > 0) + \eta(C_T < 0)} \quad \text{and} \quad \bar{A}_T = \frac{\eta(-\bar{C}_T > 0) - \eta(-\bar{C}_T < 0)}{\eta(-\bar{C}_T > 0) + \eta(-\bar{C}_T < 0)}, \tag{10}$$

$$\text{with } \mathcal{A}_{CP} = \frac{1}{2}(A_T - \bar{A}_T). \tag{11}$$

This gives the results:

```
=====
Method 1 (from fittings)
=====

yields
events          eta        err_self    err_fit
(C_T>0)       24.7322   4.9731     1.7745
(C_T<0)       35.6901   5.9741     2.7049
(-Cbar_T>0)   26.8409   5.1808     1.2939
(-Cbar_T<0)   21.3494   4.6205     0.6297

Asymmetries
A_T      errA_T      A_T_conj  errA_T_conj  a_cp      err_a_cp
-0.1814  0.1767    0.1140    0.1700    -0.1477   0.1226
```

Figure 73: The yields and asymmetries calculated from the fitted Gaussian distributions of the B^0 resonances (from Fig.72).

The Triple product asymmetries in Fig.73 were larger than the predicted values from the simulation studies in the order of 10^{-2} for 10^5 events and doesn't show any P violation due to large errors. A larger size of events would reduce the error. The results for CP asymmetry is about 100 times larger than the simulation study but is still consistent with no CP violation.

An alternative method to find the yields is to sum over the bin heights of the distribution after applying the sWeights - this is equivalent to sum over the sWeights (gives the same results). This removes the uncertainties from the fitting and only accounts for the uncertainty from the yields itself.

For all the events i with $C_{T_i} > 0$ and sWeights w_i , the yields can be written as:

$$\eta(C_T > 0) = \sum_i w_i (C_{T_i} > 0), \quad (12)$$

and similar for the situations of $C_T < 0$, $-\bar{C}_T < 0$ and $-\bar{C}_T > 0$. The asymmetries were then found by using Eq.11.

The results are:

===== Method 2 (from weights) =====						
events	eta(weights)	err_self(weights)	Asymmetries (using weights)			
(C_T>0)	25.2125	5.0212	A_T	errA_T	A_T_conj	errA_T_conj
(C_T<0)	36.5357	6.0445	-0.1834	0.1251	0.1005	0.1360
(-Cbar_T>0)	29.4434	5.4262	a_cp	err_a_cp		
(-Cbar_T<0)	24.0639	4.9055	-0.1420	0.0924		

Figure 74: The yields and asymmetries calculated from the sum of the sWeights.

Comparing this to the results in Fig.73, the asymmetries changes by 10^{-2} to 10^{-3} and the errors has been decreased by 3×10^{-2} to 5×10^{-2} .

A third attempt is to cut the un-weighted data around the B^0 resonance (i.e. at $5.2\text{-}5.35\text{ GeV}/c^2$) and assume the signal comes from the B^0 decay only. One can use this data to find the asymmetries by applying the code for studying generated data. This gives the number of events of 136 (> 115). This gives the results of asymmetries:

===== Method 3 (from cuttings) =====					
Asymmetries (cut data)					
A_T	errA_T	A_T_conj	errA_T_conj	a_cp	err_a_cp
-0.1471	0.0848	0.0909	0.0950	-0.1190	0.0637

Figure 75: The asymmetries calculated the data after cutting at 5.2 and 5.35 GeV/c^2 in the un-weighted data.

Comparing to the results in Fig.73 and Fig.74, the asymmetries are getting closer to zero and the errors drop again to show the CP asymmetry with 1.8σ . From the simulation studies, we don't expect to see any CP violation with this amount of data. The results indicates an overestimation in the data of the B^0 decay.

15 March 2020, Sunday

Previously, an analysis in the LHCb Run I data was performed. Now add the Run II (2016) data, which is 2263 data points. This add Run I together to give $2263+2678 = 4941$ events. Data from Run II(2017&2018) is yet to be analysed, which will give 3 times more data. The method used is the same as for analysing Run I. The total weighted number of data is 203.

This shows the results of fitting parameters for the B^0 resonance (Gaussian distribution) and the values of the asymmetries from three different approaches:

```

bin=100
      A      err_A     mean   err_mean sigma  err_sigma type
B0 14.7170  0.4666  5.2770  0.0006  0.0159  0.0006  B0(C_T>0)
B0 17.9906  0.4740  5.2813  0.0005  0.0169  0.0005  B0(C_T<0)
B0 9.3004   0.1271  5.2778  0.0003  0.0191  0.0003  Bbar0(-C_T>0)
B0 13.2711  0.2594  5.2832  0.0003  0.0154  0.0003  Bbar0(-C_T<0)

===== Method 1 (from fittings) =====

yields
events          eta          err_self    err_fit
(C_T>0)        48.4851      6.9631      2.3480
(C_T<0)        62.0303      7.8759      2.4964
(-Cbar_T>0)    46.6837      6.8325      0.9749
(-Cbar_T<0)    44.4360      6.6660      1.3269

Asymmetries
A_T      errA_T     A_T_conj errA_T_conj   a_cp      err_a_cp
-0.1226   0.1254    0.0247    0.1227      -0.0736   0.0877

===== Method 2 (from weights) =====

events      eta(weights)   err_self(weights)
(C_T>0)      49.4107      7.0293
(C_T<0)      62.6628      7.9160
(-Cbar_T>0)   46.5319      6.8214
(-Cbar_T<0)   44.6955      6.6855

Asymmetries (using weights)
A_T      errA_T     A_T_conj errA_T_conj   a_cp      err_a_cp
-0.1182   0.0938    0.0201    0.1047      -0.0692   0.0703

===== Method 3 (from cuttings) =====

Asymmetries (cut data)
A_T      errA_T     A_T_conj errA_T_conj   a_cp      err_a_cp
-0.1228   0.0657    0.1053    0.0721      -0.1140   0.0488

```

Figure 76: The results of the fittings and the asymmetries from three different approaches for Run I and Run II (2016) data.

It can be seen that the results from the first two approaches are getting more closer to each other for a larger number of events and the uncertainties has been reduced. The values of \bar{A}_T has been significantly reduced from 0.1 to 0.02 after adding the Run II (2016) data, but the uncertainties remains large up to $> \pm 0.1$. The values for A_T , \bar{A}_T and A_{CP} have got the larger deviations from zero compared with simulation studies. The results from the third method shows P violation with 2.75σ - this is again not expected for this number of events according to previous simulation studies, which might be due to the contribution from the noises.

17 March 2020, Tuesday

Add a little more LHCb data - this gives $2678+2263+147+65 = 5153$ events before weighting, and 304 events after weighting - doesn't observe about 400 events (as expected). It was realised that the value of opt_cut used to cut the data with particular NN_weights would only work for the Run I data previous analysed. It might not work for the Run II (2016) data and the additional data.

The values of opt_cut are different for different data files. Now backup the old files and use the new files instead. They are:

Data_sig_tos_weights-Run1.pkl	opt_cut = 0.9968
Data_sig_tos_weights-Run2.pkl	opt_cut = 0.9693
Data_sig_tis_weights-Run1.pkl	opt_cut = 0.9988
Data_sig_tis_weights-Run2.pkl	opt_cut = 0.9708

Note: [TOS (Trigger on Signal) and TIS (Trigger independent of Signal) are different categories of data. We should find out the details before you write up your report but for now don't worry about it.]

By applying the new opt_cut, the number of events before weighting is $354+395+98+190 = 1037$, and after weighting is 399. The results from the three approaches are:

```

bin=100
      A      err_A     mean   err_mean sigma  err_sigma type
B0 8.5459  0.3211  5.2811  0.0008  0.0173  0.0008    B0(C_T>0)
B0 11.2582 0.3686  5.2797  0.0006  0.0157  0.0006    B0(C_T<0)
B0 9.4059  0.3081  5.2801  0.0006  0.0157  0.0006  Bbar0(-C_T>0)
B0 9.5836  0.4312  5.2826  0.0008  0.0145  0.0008  Bbar0(-C_T<0)

===== Method 1 (from fittings) =====

yields
events          eta          err_self      err_fit
(C_T>0)        94.6734      9.7300      5.4333
(C_T<0)        120.0595     10.9572      6.0044
(-Cbar_T>0)    91.0756      9.5434      4.5575
(-Cbar_T<0)    87.3979      9.3487      6.0065

Asymmetries
A_T      errA_T      A_T_conj errA_T_conj   a_cp      err_a_cp
-0.1182  0.1053     0.0206    0.1170      -0.0694    0.0787

===== Method 2 (from weights) =====

events      eta(weights)    err_self(weights)
(C_T>0)      92.6714      9.6266
(C_T<0)      123.0599     11.0932
(-Cbar_T>0)   91.7746      9.5799
(-Cbar_T<0)   91.6202      9.5718

Asymmetries (using weights)
A_T      errA_T      A_T_conj errA_T_conj   a_cp      err_a_cp
-0.1409  0.0674     0.0008    0.0738      -0.0709    0.0500

===== Method 3 (from cuttings) =====

Asymmetries (cut data)
A_T      errA_T      A_T_conj errA_T_conj   a_cp      err_a_cp
-0.0987  0.0501     0.0435    0.0538      -0.0711    0.0367

```

Figure 77: The results of the fittings and the asymmetries from three different approaches for Run I and Run II (2016) data (new data file).

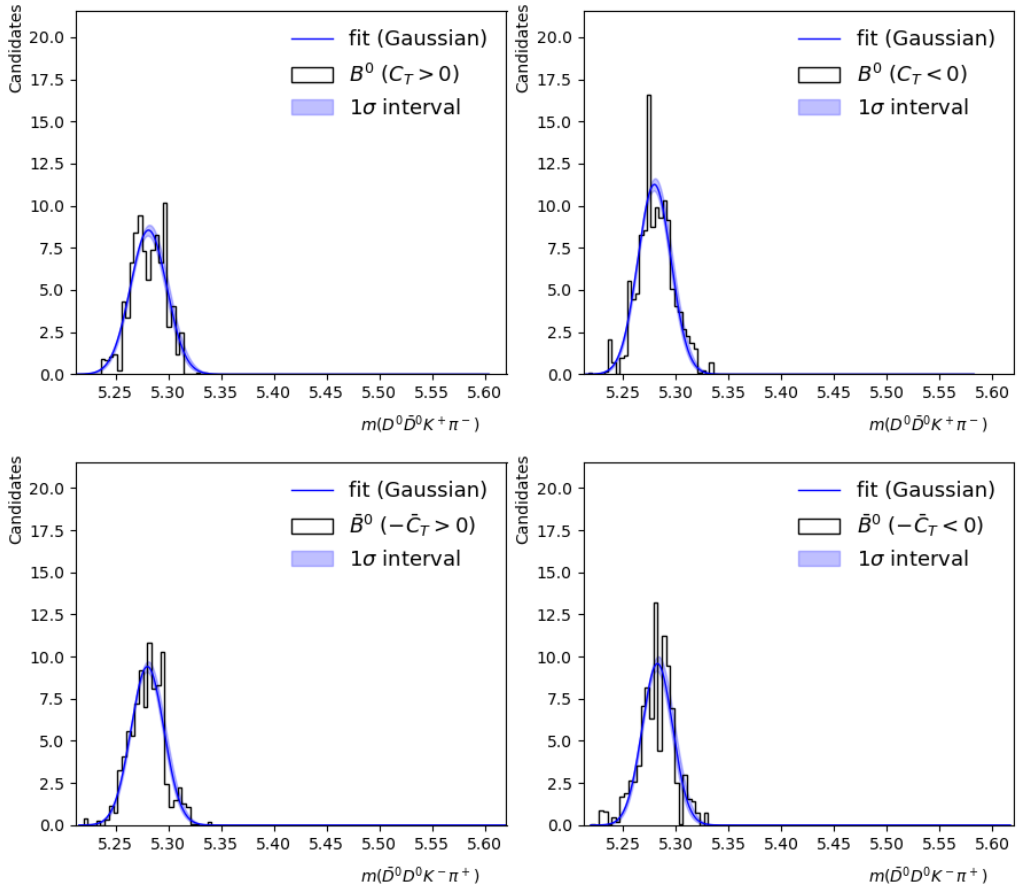


Figure 78: The fitted distribution of the B_0 resonance with showing the $1-\sigma$ tolerance for the Run I and Run II (2016) from new data files.

The distributions were also fitted by the relativistic Breit-Wigner distribution giving the results:

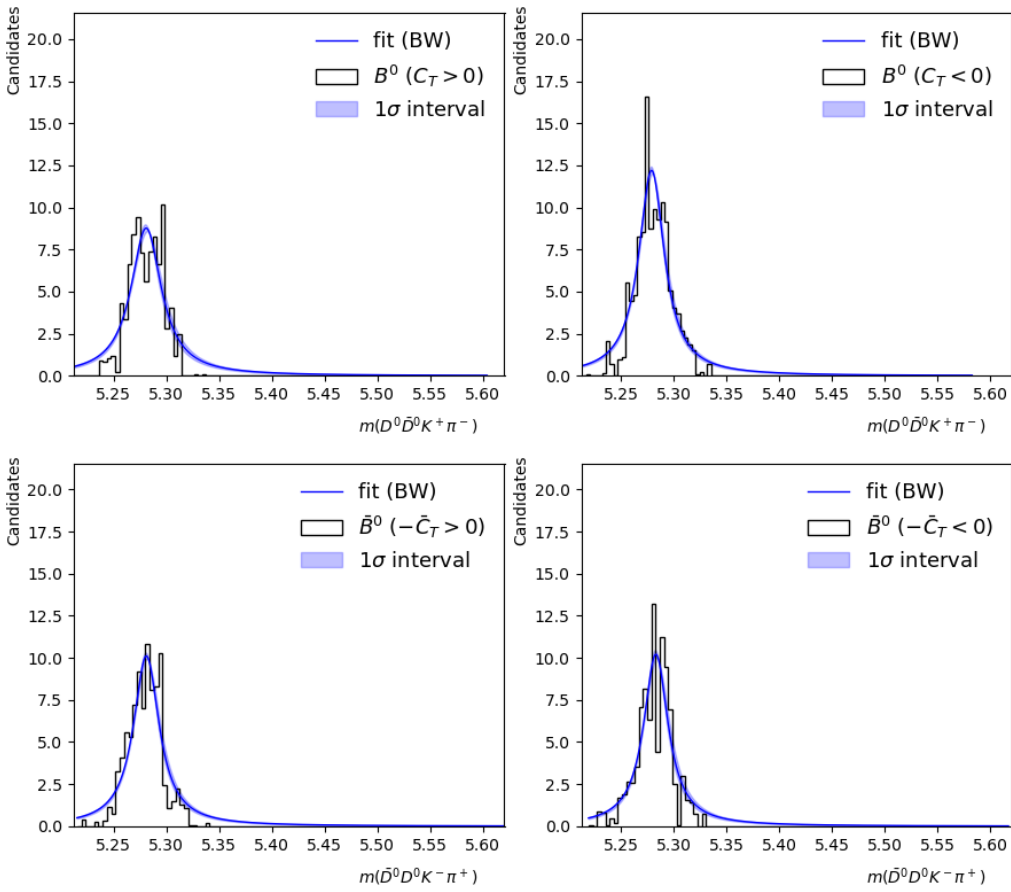


Figure 79: The fitted Breit-Wigner distribution of the B_0 resonance with showing the $1-\sigma$ tolerance for the Run I and Run II (2016) from new data files.

bin=100							
	A	err_A	E	err_E	width	err_width	type
B0	0.3946	0.0224	5.2808	0.0010	0.0353	0.0028	$B_0(C_T > 0)$
B0	0.4629	0.0200	5.2789	0.0006	0.0297	0.0018	$B_0(C_T < 0)$
B0	0.3847	0.0176	5.2810	0.0007	0.0298	0.0019	$\bar{B}^0(-C_T > 0)$
B0	0.3699	0.0207	5.2830	0.0008	0.0284	0.0023	$\bar{B}^0(-C_T < 0)$

Figure 80: The values of the fitted parameters from the Breit-Wigner distribution of the B_0 resonance for the Run I and Run II (2016) from new data files.

19 March 2020, Thursday

It's been noticed that the results are slightly different by removing the duplicated data (1% to 2% of them). I am not sure if it should be removed and why there is duplicated data?

After removing the duplicated data, the number of events before weighting is $347+390+98+190 = 1025$, and after weighting is 396.

The results are:

```

bin=100
      A     err_A     mean   err_mean sigma  err_sigma type
B0  8.5492  0.3215  5.2809  0.0007  0.0172  0.0007  B0(C_T>0)
B0 11.1967  0.3713  5.2797  0.0006  0.0157  0.0006  B0(C_T<0)
B0  9.4154  0.3091  5.2801  0.0006  0.0156  0.0006  Bbar0(-C_T>0)
B0  9.5489  0.4306  5.2828  0.0007  0.0143  0.0007  Bbar0(-C_T<0)

===== Method 1 (from fittings) =====

yields
events          eta        err_self      err_fit
(C_T>0)       93.8457    9.6874     5.3904
(C_T<0)       119.1591   10.9160    6.0361
(-Cbar_T>0)   90.9449    9.5365     4.5609
(-Cbar_T<0)   86.1737    9.2830     5.9355

Asymmetries
A_T      errA_T     A_T_conj errA_T_conj   a_cp      err_a_cp
-0.1188   0.1058    0.0269    0.1174      -0.0729   0.0790

===== Method 2 (from weights) =====

events      eta(weights)  err_self(weights)
(C_T>0)     91.9746     9.5903
(C_T<0)     121.9837   11.0446
(-Cbar_T>0) 91.4915     9.5651
(-Cbar_T<0) 90.7447     9.5260

Asymmetries (using weights)
A_T      errA_T     A_T_conj errA_T_conj   a_cp      err_a_cp
-0.1403   0.0677    0.0041    0.0741      -0.0722   0.0502

===== Method 3 (from cuttings) =====

Asymmetries (cut data)
A_T      errA_T     A_T_conj errA_T_conj   a_cp      err_a_cp
-0.0946   0.0503    0.0468    0.0540      -0.0707   0.0369

```

Figure 81: The results of the fittings and the asymmetries from three different approaches for Run I and Run II (2016) data (new data file) after removing the duplicated data.